

Behaviour of High Rise Building under Accidental Loading

Hrishikesh Jejurkar¹, Prof. S.A. Mishra²

¹M. Tech Student (Structures)

²Prof. (Civil Dept.)

Submitted: 01-08-2022

Revised: 07-08-2022

Accepted: 10-08-2022

ABSTRACT:

Accidental loads such as explosion and vehicle impact could lead to failure of one or several load-bearing members in the structures, which is likely to trigger disproportionate progressive collapse of overall structures. A bomb explosion within or immediately nearby a building can cause catastrophic damage on the building's external and internal structural frames, collapsing of walls, blowing out of large expanses of windows, and shutting down of critical life-safety systems. Loss of life and injuries to occupants can result from many causes, including direct blast-effects, structural collapse, debris impact, fire, and smoke. The indirect effects can combine to inhibit or prevent timely evacuation, thereby contributing to additional casualties.

In addition, major catastrophes resulting from gas-chemical explosions result in large dynamic loads, greater than the original design loads, of many structures. Due to the threat from such extreme loading conditions, efforts have been made during the past three decades to develop methods of structural analysis and design to resist blast loads. The interest is for building safety with regards to such highly dynamic events after the recent decades of terrorist attacks. The interest has expanded from civil defence shelters and pure military targets to also include civil buildings used for different civil functions.

Studies were conducted on the behaviour of structural concrete subjected to blast loads. These studies gradually enhanced the understanding of the role that structural details play in affecting the behaviour. The response of simple RC building subjected to constant axial loads and lateral blast loads was examined. The finite element package ANSYS was used to model RC building with different boundary conditions and using the mesh less method to reduce mesh distortions.

ACKNOWLEDGMENT

Words are inadequate to express my deep sense of gratitude to my guide Prof. S. A. Mishra (M.Tech co-ordinator), for consistent guidance and inspiration throughout the project work, which I am sure, will go a long in my life.

I am also owe sincere thanks to Dr. R. A. Dubal, Head of Civil Engineering Department and all civil department staff of Rajarshi Shahu College of Engineering, Tathawade, who have rendered their invaluable support and guidance for carrying out this project work successfully.

Last but not least, I express my deep sense of gratitude to my family and friends and all those who have helped me directly or indirectly for their constant support and motivation throughout the course of this project work.

I. INTRODUCTION

1.1 General

For decades the focus of civil defense has been on civil defense shelters to withstand the threat against warfare and to protect civilians. Later years, the general focus has often shifted towards the protection of specific targets which host important functions to society. Direct attacks towards the civil population, such as terrorist attacks, also pose a more common threat today than for a few years ago. Due to the rather rapid shift of area of interest, the general engineering community lack much of the knowledge and tools to design and evaluate structures with respect to dynamic events with very fast transient and high magnitude peak loads. Most structural analysis approaches have been developed with different simplifications and approximations, because of limitations in knowledge and to restrict the extent of cases studied. When it comes to response of concrete structures due to highly dynamic events, the load due to an explosion and the general response of statically loaded concrete structures are relatively well-known. However, despite decades of research

within the area, many phenomena involved for the dynamic response of reinforced concrete structures are not yet fully understood. Numerical modelling of dynamic events has been more common in recent years and is to a large extent treated as an available complement to physical testing. Even so, the tools and techniques to evaluate structures with numerical models are in many respects unexplored. Since some phenomena are not fully understood, it becomes rather complicated to determine the needed properties of these numerical models. Due to different accidental or intentional events, the behavior of structural components subjected to blast loading has been the subject of considerable research effort in recent years. Conventional structures, particularly that above grade, normally are not designed to resist blast loads; and because the magnitudes of design loads are significantly lower than those produced by most explosions, conventional structures are susceptible to damage from explosions. With this in mind, developers, architects and engineers increasingly are seeking solutions for potential blast situations, to protect building occupants and the structures.

1.2 Background

1.2.1 Phenomenon of explosion and blast

In general, an explosion is the result of a very rapid release of large amounts of energy within a limited space. Explosions can be categorized on the basis of their nature as physical, nuclear and chemical events.

In physical explosion: - Energy may be released from the catastrophic failure of a cylinder of a compressed gas, volcanic eruption or even mixing of two liquids at different temperature.

In nuclear explosion: - Energy is released from the formation of different atomic nuclei by the redistribution of the protons and neutrons within the inner acting nuclei.

In chemical explosion: - The rapid oxidation of the fuel elements (carbon and hydrogen atoms) is the main source of energy.

The type of burst mainly classified as

a. Air burst

- b. High altitude burst
- c. Under water burst
- d. Undergroundburst
- e. Surfaceburst

The discussion in this section is limited to air burst or surface burst. This information is then used to determine the dynamic loads on surface structures that are subjected to such blast pressures and to design them accordingly. It should be pointed out that surface structure cannot be protected from a direct hit by a nuclear bomb; it can however, be designed to resist the blast pressures when it is located at some distance from the point of burst. The destructive action of nuclear weapon is much more severe than that of a conventional weapon and is due to blast or shock. In a typical air burst at an altitude below 100,000 ft. an approximate distribution of energy would consist of 50% blast and shock, 35% thermal radiation, 10% residual nuclear radiation and 5% initial nuclear radiation.

The sudden release of energy initiates a pressure wave in the surrounding medium, known as a shock wave as shown in Fig.1.1 (a). When an explosion takes place, the expansion of the hot gases produces a pressure wave in the surrounding air. As this wave moves away from the centre of explosion, the inner part moves through the region that was previously compressed and is now heated by the leading part of the wave. As the pressure wave moves with the velocity of sound, the temperature is about 3000°-4000°C and the pressure is nearly 300 kilobar of the air causing this velocity to increase. The inner part of the wave starts to move faster and gradually overtakes the leading part of the waves. After a short period of time the pressure wave front becomes abrupt, thus forming a shock front somewhat similar to Fig.1.1(b). The maximum overpressure occurs at the shock front and is called the peak overpressure. Behind the shock front, the overpressure drops very rapidly to about one-half the peak overpressure and remains almost uniform in the central region of the explosion.

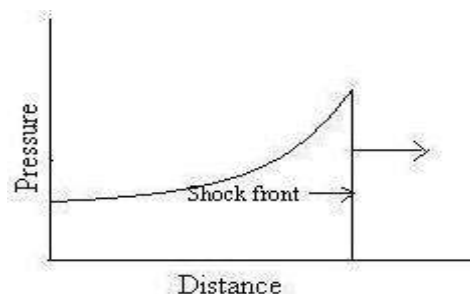


Fig.1.1(a) Variation of pressure with distance

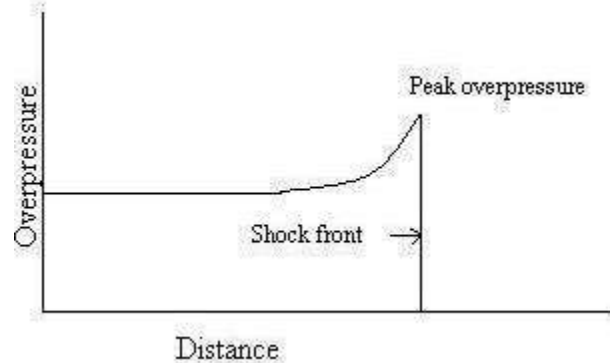


Fig.1.1(b) Formation of shock front in a shock wave.

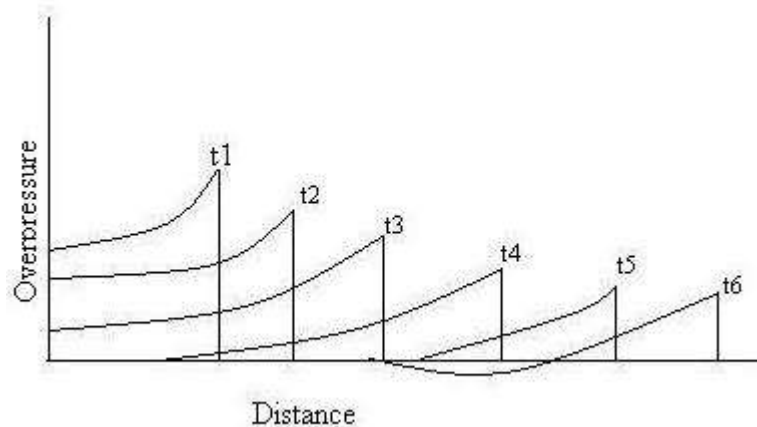


Fig.1.1(c) Variation of overpressure with distance from center of explosion at various times.

An expansion proceeds, the overpressure in the shock front decreases steadily; the pressure behind the front does not remain constant, but instead, fall off in a regular manner. After a short time, at a certain distance from the centre of explosion, the pressure behind the shock front becomes smaller than that of the surrounding atmosphere and so called negative-phase or suction. The front of the blast waves weakens as it

progresses outward, and its velocity drops towards the velocity of the sound in the undisturbed atmosphere. This sequence of events is shown in Fig.1.1(c), the overpressure at time t_1, t_2, \dots, t_6 are indicated. In the curves marked t_1 to t_5 , the pressure in the blast has not fallen below that of the atmosphere. In the curve t_6 at some distance behind the shock front, the overpressure becomes negative. This is better illustrated in Fig.1.2 (a).

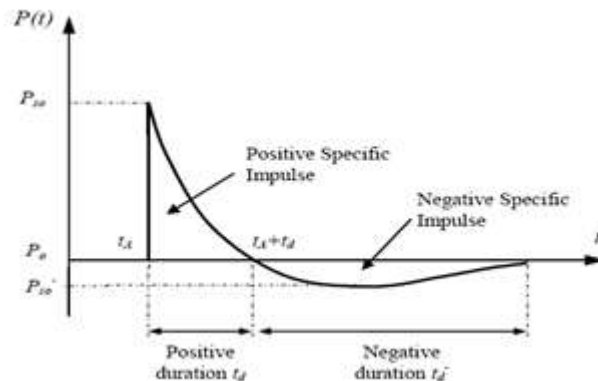


Fig.1.2(a) The variation of overpressure with distance at a given time from center of explosion.

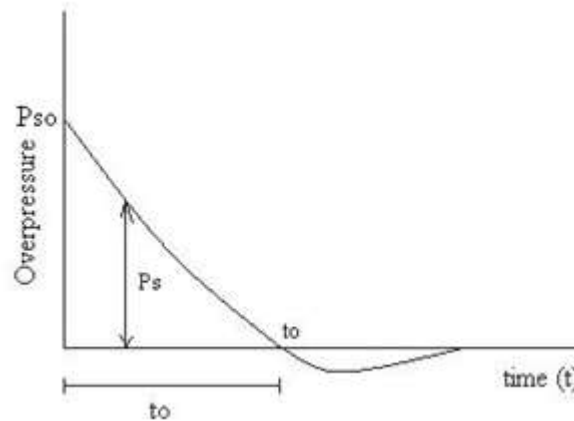


Fig.1.2(b) Variation of overpressure with

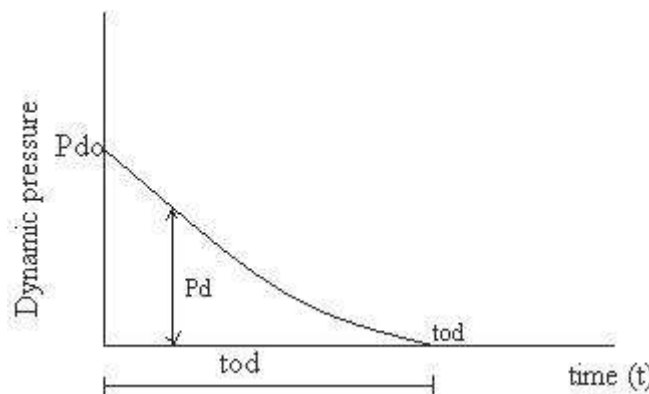


Fig.1.2(c) Variation of dynamic pressure with distance at a time from the explosion.

Time variation of the same blast wave at a given distance from the explosion is shown in Fig.1.2(b); t_o indicates the time duration of the positive phase and also the time at the end of the positive phase. Another quantity of the equivalent importance is the force that is developed from the strong winds accompanying the blast wave known as the dynamic pressure; this is proportional to the square of the wind velocity and the density of the air behind the shock

front. Its variation at a given distance from the explosion is shown in Fig.1.2(c).

Mathematically the dynamic pressure P_d is expressed as

$$P_d = \frac{1}{2} \rho u^2$$

Where u is the velocity of the air particle and ρ is the air density

The peak dynamic pressure decreases with increasing distance from the center of explosion, but the rate of decrease is different from that of the peak overpressure. At a given distance from the explosion, the time variation of the dynamic P_d behind the shock front is somewhat similar to that of the overpressure P_s , but the rate of decrease is usually different. For design purposes, the negative phase of the overpressure in Fig.1.2 (b) is not important and can be ignored.

1.2.2 Explosive air blast loading

The threat for a conventional bomb is defined by two equally important elements, the bomb size, or charge weight W , and the stand-off distance (R) between the blast source and the target (Fig.1.4). For example, the blast occurred at the basement of World Trade Centre in 1993 has the charge weight of 816.5 kg TNT. The Oklahoma bomb in 1995 has a charge weight of 1814 kg at a stand-off of 5m [13]. A terrorist attack may range from the small letter bomb to the gigantic truck bomb as experienced in Oklahoma City, the mechanics of a conventional explosion and their effects on a target must be addressed.

Throughout the pressure-time profile, two main phases can be observed; portion above ambient is scaled positive phase of duration

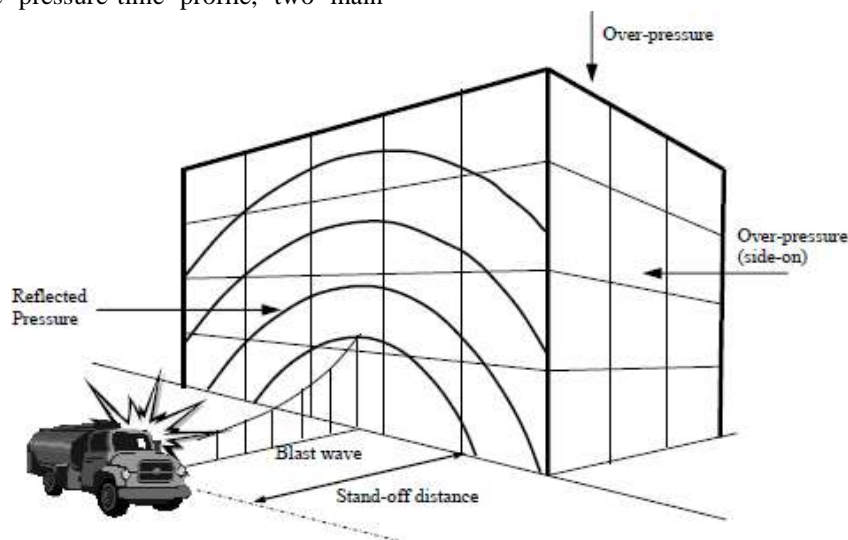


Figure 1.4: Blast Loads on a Building

If the exterior building walls are capable of resisting the blast load, the shock front penetrates through window and door openings, subjecting the floors, ceilings, walls, contents, and people to sudden pressures and fragments from shattered windows, doors, etc. Building components not capable of resisting the blast wave will fracture and be further fragmented and moved by the dynamic

pressure that immediately follows the shock front. Building contents and people will be displaced and tumbled in the direction of blast wave propagation. In this manner the blast will propagate through the building.

STAND-OFF DISTANCE

Stand-off distance refers to the direct, unobstructed distance between a weapon and its target.

HEIGHT OF BURST (HOB)

Height of burst refers to aerial attacks. It is the direct distance between the exploding weapon in the air and the target.

pressure that immediately follows the shock front. Building contents and people will be displaced and tumbled in the direction of blast wave propagation. In this manner the blast will propagate through the building.

1.2.2 A) BLAST WAVE SCALING LAWS

All blast parameters are primarily

dependent on the amount of energy released by a detonation in the form of a blast wave and the distance from the explosion. A universal normalized description of the blast effects can be given by scaling distance relative to $(E/P_0)^{1/3}$ and scaling pressure relative to P_0 , where E is the energy release (kJ) and P_0 the ambient pressure (typically 100 kN/m²). For convenience, however, it is general practice to express the basic explosive input or charge weight W as an equivalent mass of TNT. Results are then given as a function of the dimensional distance parameter,

$$\text{Scaled Distance} \propto Z \propto \frac{R}{W^{1/3}} \quad \dots \quad (2)$$

Where R is the actual effective distance from the explosion.
 W is generally expressed in kilograms.

Scaling laws provide parametric correlations between a particular explosion and a standard charge of the same substance.

1.2.2 B) PREDICTION OF BLAST PRESSURE

Blast wave parameter for conventional high explosive materials have been the focus of a number of studies during the 1950's and 1960's. The estimations of peak overpressure due to spherical blast based on scaled distance $Z=R/W^{1/3}$ was introduced by Brode (1955) as:

$$P_{so} = \frac{6.7}{Z^2} + 1 \text{ bar} \quad (P_{so} > 10 \text{ bar}) \quad \dots \quad (3.a)$$

$$P_{so} = \frac{0.975}{Z} - \frac{1.455}{Z^2} + \frac{1.585}{Z^3} - 0.019 \text{ bar} \quad (0.1 < P_{so} < 10 \text{ bar}) \quad \dots \quad (3.b)$$

In 1961, Newmark and Hansen introduced a relationship to calculate the maximum blast pressure (P_{so}), in bars, for a high explosive charge detonates at the ground surface as:

$$P_{so} = 6784 \left(\frac{W}{R} \right)^{3+93 \left(\frac{W}{R} \right)^{1/2}} \quad \dots \quad (4)$$

In 1987, Mills introduces another expression of the peak overpressure in kpa, in which W is the equivalent charge weight in kilograms of TNT and Z is the scaled distance.

$$P_{so} = \frac{1772}{Z^3} - \frac{114}{Z^2} + \frac{108}{Z} \quad \dots \quad (5)$$

As the blast wave propagates through the atmosphere, the air behind the shock front is moving outward at lower velocity. The velocity of the air particles, and hence the wind pressure, depends on the peak overpressure of the blast wave. This later velocity of the air is associated with the dynamic pressure, $q(t)$. The maximum value, $q(s)$, say, is given by

$$q(s) = 5 P_{so}^2 / 2 (P_{so} + 7 P_0) \quad (6)$$

If the blast wave encounters an obstacle perpendicular to the direction of propagation, reflection increases the overpressure to a maximum reflected pressure P_r as:

$$P_r = 2 P_{so} \left\{ \frac{7 P_0 + 4 P_{so}}{7 P_0 + P_{so}} \right\} \quad \dots \quad (7)$$

A full discussion and extensive charts for predicting blast pressures and blast durations are given by Mays and Smith (1995) and TM5-1300 (1990). Some representative numerical values of peak reflected overpressure are given in Table 1.1.

Table No.1.1. Peak reflected overpressures P_r (in MPa) with different W - R combinations

W/R	100kg TNT	500kg TNT	1000kg TNT	2000kg TNT
1m	165.8	354.5	464.5	602.9
2.5m	34.2	89.4	130.8	188.4
5m	6.65	24.8	39.5	60.19
10m	0.85	4.25	8.15	14.7
15m	0.27	1.25	2.53	5.01
20m	0.14	0.54	1.06	2.13

25m	0.09	0.29	0.55	1.08
30m	0.06	0.19	0.33	0.63

For design purposes, reflected overpressure can be idealized by an equivalent triangular pulse of maximum peak pressure P_r and time duration t_d , which yields the reflected impulse (i_r).

$$\text{Reflected Impulse}(i_r) = \frac{1}{2} P_r t_d$$

Duration t_d is related directly to the time taken for the overpressure to be dissipated. Overpressure arising from wave reflection dissipates as the perturbation propagates to the edges of the obstacle at a velocity related to the speed of sound (U_s) in the compressed and heated air behind the wave front. Denoting the maximum distance from an edge as S (for example, the lesser of the height or half the width of a conventional building), the additional pressure due to reflection is considered to reduce from $P_r - P_{s0}$ to zero in time $3S/U_s$. Conservatively, U_s can be taken as the normal speed of sound, which is about 340 m/s, and the additional impulse to the structure evaluated on the assumption of a linear decay. After the blast wave has passed the rear corner of a prismatic obstacle, the pressure similarly propagates on to the rear face; linear build-up over duration $5S/U_s$ has been suggested. For skeletal structures the effective duration of the net overpressure load is thus small, and the drag loading based on the dynamic pressure is then likely to be dominant. Conventional wind-loading pressure coefficients may be used, with the conservative assumption of instantaneous build-up when the wave passes the plane of the relevant face of the building, the loads on the front and rear faces being numerically cumulative for the overall load effect on the structure. Various formulations have been put forward for the rate of decay of the dynamic pressure loading; a parabolic decay (i.e. corresponding to a linear decay of equivalent wind velocity) over a time equal to the total duration of positive overpressure is a practical approximation.

1.2.3 Structural Response to Blast Loading

Complexity in analyzing the dynamic response of blast-loaded structures involves the effect of high strain rates, the non-linear inelastic material behavior, the uncertainties of blast load calculations and the time-dependent deformations. Therefore, to simplify the analysis, a number of assumptions related to the response of structures and the loads has been proposed and widely accepted. To establish the principles of this

analysis, the structure is idealized as a single degree of freedom (SDOF) system and the link between the positive duration of the blast load and the natural period of vibration of the structure is established. This leads to blast load idealization and simplifies the classification of the blast loading regimes.

1.2.4 Blast Loading:

Simply put, it is the load applied to a structure from a blast wave that comes immediately after an explosion. It is the combination of overpressure and either impulse or duration. A high blast load can cause catastrophic damage to a building, both internally and externally, and can be fatal to building occupants.

A blast load determines the building's response, which tells you the damage level to expect after an explosion. Response levels have been defined by the American Society of Civil Engineers (ASCE) as Low, Medium, and High, corresponding to the amount of damage observed after a blast event. For example:

- Low response - the building may have a small amount of damage, but can still be used. There may be repairs required to ensure the structural envelope is intact.
- Medium response - the building will have widespread damage and can not be used until it is repaired. The cost of repairs may be significant.
- High response - the building's structural integrity is compromised and it may collapse. The cost of repairs will be similar to the total replacement of the building. High response buildings should not be used by occupants in a hazardous area, since severe injury or loss of life is possible.

1.3 Aim

To Analyse the behavior of high-rise building under progressive collapse under blast loading using ANSYS & Etabs.

1.3 Objectives

- Analysing the behavior of G+15, G+18, G+24 building under Blast loads.
- To calculate blast pressure intensity for 100kg TNT by using scaling law.
- To Run the same Analysis on Ansys to determine the pressure with respect to the time in sec's
- Analyzing the Response of the building of different height for the same blast pressure

intensity using Time-History Analysis on Etabs.

- Computing responses for four load combinations with respect to DL,LL,WIND & Time history.
- Comparison of variation in storey displacement, drift, stiffness, mass participation and time period

1.5 Scope of work

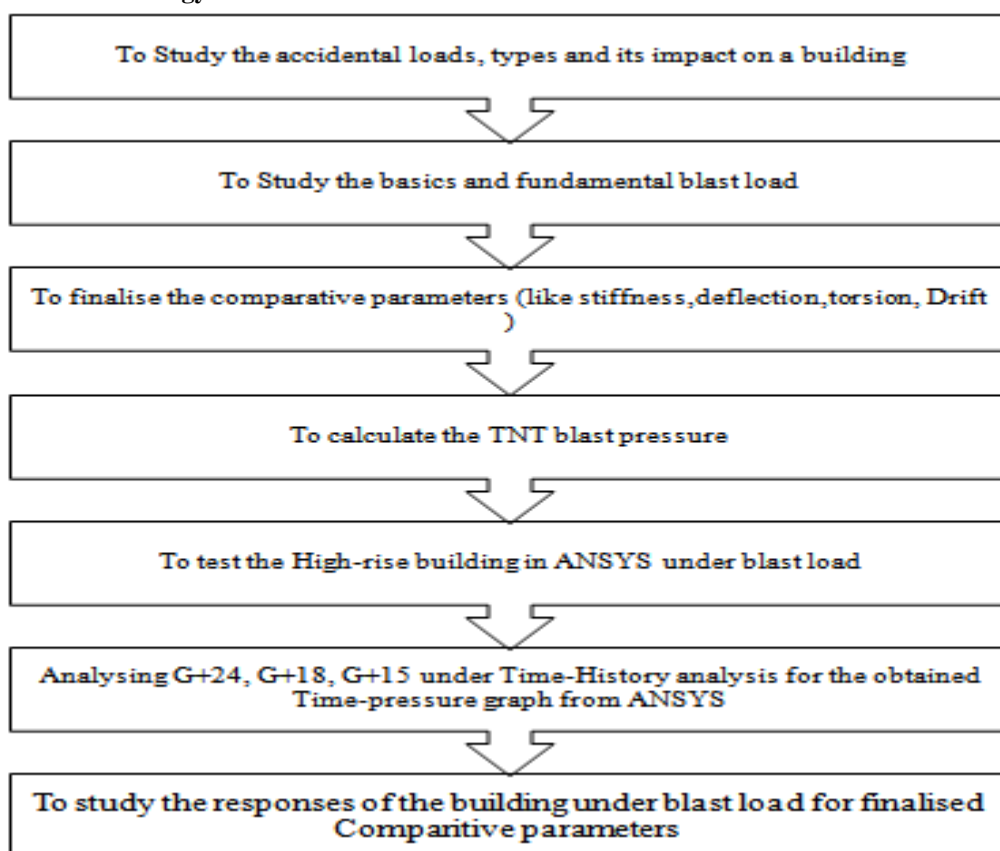
To meet the above objective, the research work plan has been focussed on the following:

- Approach towards Computation of the blast loading on a High Rise the building.
- Remedial measures to counteract the effects of blast on a building.
- Modelling of a simple RC building in ANSYS.
- Response of a simple RC building under the Blast loading in Etabs

1.6 Limitation

- Experimental studies are not carried out, only numerical and analytical model study is done

1.7 Research Methodology



II. LITERATURE REVIEW

1. Prediction of blast loading and its impact on buildings, By NITESH N. MOON, ASCE,

The response of simple RC columns subjected to constant axial loads and lateral blast loads was examined. The finite element package ANSYS was used to model RC column with different boundary conditions and using the mesh less method to reduce mesh distortions. For the response calculations, a constant axial force was first applied to the column and the equilibrium state was determined. Next, a short duration, lateral blast load was applied and the response time history was calculated. The analysis and design of structures

subjected to blast loads require a detailed understanding of blast phenomena and the dynamic response of various structural elements. This gives a comprehensive overview of the effects of explosion on structures.

2. Prediction Concrete Structures Subjected to Blast Loading Fracture due to dynamic response, Division of Structural Engineering, CHALMERS UNIVERSITY OF TECHNOLOGY G"oteborg, Sweden 2015

In the first study the response in a concrete wall subjected to shock wave blast, leading to spalling failure was investigated. This situation is important since spalled-off fragments in protective

structures may cause severe injury to the persons or equipment it is supposed to protect. Previous research indicates that spalling occurs when and where the tensile strength of a strain-softening material like concrete is reached. By using a simple uni-axial numerical model, this study shows that spalling instead occurs when the cyclic response from a blast wave gradually increase the inelastic strains in the concrete. This means that spalling takes place after several loading cycles and not necessarily at the depth where tensile strength is firstly reached. Furthermore, the study shows that the cyclic response in the material model used for numerical simulation has a decisive influence on the position and extent of the resulting spalling crack.

3. Response of buildings exposed to blast load method evaluation, by CARL LÖFQUIST, 2016 Division of Structural Mechanics, Faculty of Engineering LTH, Lund University, Sweden. Printed by Media-Tryck LU, Lund, Sweden, October 2016

The purpose of this Master thesis is to investigate and develop dynamic models that combines sufficient accuracy with computational efficiency for structures effected by blast wave loads due to explosions. This is achieved by analysing two cases where the blast wave load is handled differently. First case handles the load as a triangular pulse load and the second case handles the load by transforming it into velocities according to the impulse and moment laws, and set as initial values when solving it as a free vibration problem. These cases are modeled in a full model and a model reduced with Ritz vectors.

4. A review of methods for predicting bomb blast effects on buildings by Alexander M. Remennikov, (2003) Journal of battlefield technology, vol 6, no 3. pp 155-161.

Study shows the methods for predicting bomb blast effects on buildings. When a single building is subjected to blast loading produced by the detonation of high explosive device. Simplified analytical techniques used for obtaining conservative estimates of the blast effects on buildings. Numerical techniques including Lagrangian, Eulerian, EulerFCT, ALE, and finite element modelling used for accurate prediction of blast loads on commercial and public buildings.

5. Column load balancing in prestressed concrete building, By S. L. Lee,¹ Fellow, ASCE, S. Tumilar,² Member, ASCE, and H. C. Chin³

Architectural and structural considerations in the design of the 27- story Wisma Dharmala office complex in Jakarta lead to the deployment of twin column clusters around the perimeter and interior of the tower block. Due to the large difference in axial loads between the twin columns, excessive differential axial shortening between the columns and high shear stresses in the connecting horizontal structural components are expected. To mitigate this condition, the column load balancing method is proposed, in which the cable profiles in the prestressed girders are designed not only for moment balancing but also to transfer evenly the shear forces in the girders to the twin columns in each cluster. The effect of load balancing is examined in this paper with the use of a simple analytical model. The predicted loads on the columns are also checked against field measurements taken from three pairs of twin columns from the time the columns are cast until the casting of the helipad floor.

6. Serviceability Performance of Prestressed Concrete Buildings Taking into Account Long Term Behaviour and Construction Sequence H. L. YIP, F. T. K. AU, S. T. SMITH

A common problem faced by engineers nowadays is the restriction on structural member dimensions due to architectural and spatial concerns. Such restrictions have resulted in the use of high strength concrete in vertical members to reduce sizes, the use of central core walls and peripheral columns to increase window areas, and the use of prestressed floors to increase spans, to name a few. Serviceability problems (e.g., cracking) may, however, arise in the long term. This paper in turn addresses two major issues associated with buildings. Firstly, the differential axial shortening between core walls and columns caused by large differences in stress levels induces additional stresses and strains in horizontal structural members, which are not normally accounted for by traditional design methods. Secondly, the post-tensioning of concrete floors gives rise to additional internal forces induced by several means such as sequential construction, and secondary "P-" effects of the high-strength slender columns. As it is almost impossible to eliminate these secondary effects completely, a series of studies have been carried out to examine their effects on the structural design of these buildings.

7. The analysis of prestressed concrete structures and the application of recent research by peter beaumontmorice, b.sc., ph.d., a.m.i.c.e.

The Paper illustrates the application of some results of recent research on the behaviour of prestressed concrete structures. A simple set of expressions is developed for the elastic design and ultimate load-carrying capacity of prestressed members in both statically determinate and indeterminate structures. The use of these expressions in the analysis of continuous beams, portal frames, and bridge decks is discussed in the light of the results of experimental work. Some aspects of research on the effects of friction between prestressing tendons and their ducts in post-tensioned members are included, together with the principal results of a study of the transmission length in factory-made pretensioned units.

8. Experimental and numerical study on the performance of externally prestressed reinforced high strength concrete beams with openings Ahmed M. El-Basouny¹, Hamed S. Askar¹ Mohamad E, El-Zoughiby

This study investigates experimentally and numerically the performance of externally prestressed reinforced high strength concrete (HSC) beams with central openings. Seven externally prestressed rectangular HSC beams (six with central openings and a reference solid beam) are loaded incrementally to failure. All the beams have the same dimensions, reinforcement ratio and openings of variable size. Experimentally, the results show that, the appearance of the first flexural crack and the flexural stiffness reduction are largely governed by opening height. In contrast, the opening length greatly affects the presence of the first shear crack and the obtained values of strains in stirrups. Additionally, the opening length and height when combined can affect the strains in top- and bottom-bars and the failure load of the test beams. Numerically, a three-dimensional nonlinear finite element analysis using ANSYS has been carried-out to analyze seventy (70) externally prestressed HSC beams with central openings. Based on the numerical results, a general formula to predict the ultimate moment is generated and verified. It can be used to predict the load carrying capacity of aging concrete elements with openings retrofitted using external prestressing techniques

9. Building structure failures caused by accidental loads

The paper presents the characteristics of abnormal loads and the recommendations adopted for structural design to prevent constructions from

disproportionate damage and to limit the consequences of accidental loads in compliance with Eurocode 1 PN-EN 1991-1-7. The article describes progressive collapses and analyses the construction of two buildings: the Murrah Federal Building in Oklahoma and the Pentagon Building in Washington.

10. Accidental Eccentricity of Story Shear for Low-Rise Office Buildings Jaime De-la-Colina; Bernardino Benítez; and Sonia E. Ruiz

This paper presents the results of a Monte Carlo simulation study on accidental eccentricity of low-rise office buildings. The study incorporates results of a live-load survey in several office buildings in Mexico City. Probability density functions (PDF) for both intensity and position of live load are initially obtained from this survey. These PDFs are used in the simulation procedure. Additionally, the position and intensity of dead load as well as the stiffness of lateral resisting elements are assumed to be random. Stiffness among columns is assumed to be uncorrelated. Five- and 10-story building models with square and rectangular plans are used. For each case, three types of slabs are included in order to account for different live-load to dead-load ratios. This study shows the effect of the following variables on the estimation of accidental eccentricities: vertical location of the story in the building, dead-load to live-load ratio, number of columns in a story, and the direction of analysis in rectangular plans.

11. Estimation of Accidental Torsion Effects for Seismic Design of Buildings Juan C. De la Llera, Anil K. Chopra,

This paper presents the results of a Monte Carlo simulation study on accidental eccentricity of low-rise office buildings. The study incorporates results of a live-load survey in several office buildings in Mexico City. Probability density functions (PDF) for both intensity and position of live load are initially obtained from this survey. These PDFs are used in the simulation procedure. Additionally, the position and intensity of dead load as well as the stiffness of lateral resisting elements are assumed to be random. Stiffness among columns is assumed to be uncorrelated. Five- and 10-story building models with square and rectangular plans are used. For each case, three types of slabs are included in order to account for different live-load to dead-load ratios. This study shows the effect of the following variables on the estimation of accidental eccentricities: vertical location of the story in the building, dead-load to

live-load ratio, number of columns in a story, and the direction of analysis in rectangular plans.

12. Determining Appropriate Design Impact Loads to Roadside Structures Using Stochastic

Modeling Ivar Björnsson; Sven Thelandersson; and Fredrik Carlsson

The design and verification of built structures requires structural engineers to consider accidental loading situations. The accidental loading situation investigated in this paper is heavy-goods vehicle (HGV) collisions with roadside structures; focus is on the design of bridge-supporting structures. The impact loads were determined from Monte Carlo simulations of a probabilistic model in which highway traffic measurements and accident statistics in Sweden are input. These loads were calculated for structures adjacent to straight roads as well as roads with curvature, and include considerations of the directional load components. Comparisons were made between the simulation results and approaches given in design codes, with focus on the Eurocode. The simplified approaches provided in the code were inadequate in their treatment of these design situations. Alternative equations for calculating impact forces and energies are presented. These equations can be used for determining design values for impact forces or for conducting probability/risk-based assessments of bridge supports subjected to HGV impacts. In this way, a more consistent treatment of HGV impacts in the design of bridge structures is achieved

13. Jun Yu; Tassilo Rinder; Alexander Stolz; Kang-Hai Tan, Dynamic Progressive Collapse of an RC Assemblage Induced by Contact Detonation (2008)

The nature of progressive collapse is a dynamic event caused by accidental or intentional extraordinary loading. Most published experimental programs are conducted statically, without any consideration of the accidental loading and treating progressive collapse as threat independent. This paper demonstrates the more realistic process of progressive collapse in an experimental program on reinforced concrete sub assemblages collapsed by a combination of dead weight loading and contact detonation. The dynamic results are represented systematically at different aspects and compared with previous published quasi-static experiments in terms of structural mechanisms, crack patterns and local failure modes. Moreover, the dynamic increase factor (DIF) of reinforcing bars and the dynamic

load amplification factor (DLAF) are investigated and discussed. Following the above comparisons and the findings in the dynamic tests, previous quasi-static test results can be linked to actual progressive collapse behaviour more convincingly. Finally, the dynamic tests also highlight the effect of contact detonation on structures, which are often not considered in quasi-static tests and design guidelines. The test results indicate that contact detonation causes uplift and out-of-plane actions to the sub assemblage before their downward movement under gravity load, in which the strain rate of reinforcement is between 10^{-2} and 10^{-1} /s. Moreover, the structural mechanisms are similar in both quasi-static and dynamic tests

14. Youpo Su, Ying Tian, University of Nevada, Las Vegas, Progressive Collapse Resistance of Axially-Restrained Frame Beams, Aci Structural Journal 106(5):600-607, September (2009)

Twelve specimens representing reinforced concrete frame beams were tested to investigate their gravity load-carrying capacity against progressive collapse. In these tests, the beams within the frame subassemblies were restrained longitudinally against axial deformation. The tests indicated that the compressive arch action due to longitudinal restraint can significantly enhance the flexural strength of a beam subjected to vertical loads. The compressive arch action was observed to be a function of flexural reinforcement ratio and ratio of beam span to depth. The test results validated an analytical model that has considered the axial restraining effects on beam loading capacity. The application of compressive arch effect to the prevention of progressive collapse is discussed.

15. Meng-Hao Tsai, Effect of Interior Brick-infill Partitions on the Progressive Collapse Potential of a RC Building: Linear Static Analysis Results Article, February (2009)

Interior brick-infill partitions are usually considered as non-structural components, and only their weight is accounted for in practical structural design. In this study, the brick-infill panels are simulated by compression struts to clarify their effect on the progressive collapse potential of an earthquake-resistant RC building. Three-dimensional finite element models are constructed for the RC building subjected to sudden column loss. Linear static analyses are conducted to investigate the variation of demand-to-capacity ratio (DCR) of beam-end moment and the axial

force variation of the beams adjacent to the removed column. Study results indicate that the brick-infill effect depends on their location with respect to the removed column. As they are filled in a structural bay with a shorter span adjacent to the column-removed line, more significant reduction of DCR may be achieved. However, under certain conditions, the brick infill may increase the axial tension of the two-span beam bridging the removed column.

16. Ahmed Atta and Mohamed Taman, Using high-performance cementitious mortar and external prestressing for retrofitting of corroded reinforced concrete beams, Advances in Structural Engineering (2020)

The effect of using high-performance polypropylene fiber-reinforced cementitious mortar on reinforced concrete beam repair was presented in this article. Results of an experimental study for the flexural performance of 13 reinforced concrete beams were presented. The corrosion level, in terms of the mass loss of steel, was estimated to be 10% and 15%. Three non-strengthened specimens were tested as a reference: one control uncorroded specimen and two control specimens corroded with 10% and 15%. Ten specimens were strengthened using different techniques; replacement of the spilled concrete at the tension zone with 40-mm-thick high-performance polypropylene fiber-reinforced cementitious mortar, using external prestressing bars at the tension zone with adding 20-mm-thick high-performance polypropylene fiber-reinforced cementitious mortar at the compression zone, and a combination of these techniques. The prestressing reinforcing bars stress was chosen to be 0.25fpy and 0.38fpy for the corroded 10% specimens and 0.25fpy for the corroded 15% specimens. A combination of 40-mm-thick high-performance polypropylene fiber-reinforced cementitious mortar at the tension side and external prestressing bars at the tension zone increased the specimen capacity by 15% and 34% compared with the uncorroded and 10% corroded control specimens, respectively. A comparative study was conducted to evaluate the efficiency of various strengthening techniques. An analytical model was proposed in order to give design guidelines.

17. V. Kumar, M. A. Iqbal", A. K. Mittalb, Behaviour of prestressed concrete under drop impact loading, 11th International Symposium on Plasticity and Impact Mechanics, 20 (2017)

Structures are subjected to impacts loads of low to high intensity such as developed from

falling of heavy object on floors, vehicle accident with bridge columns, missile attacks during war and terrorist blasts etc. The time duration under such incident is very low. an order of few milliseconds; therefore, local and global deformation behaviour of structures was of great importance in past research. Moreover, under impact loading the material behaviour is entirely different than under static loading conditions. Therefore, in this study, impact tests have been carried out on prestressed concrete plates to identify their behaviour when subjected to drop weight impact. The prestressed concrete plates of size 0.8 m x 0.8 m and thickness 100 mm were subjected to drop impact by 242.8 kg hammer. These plates having identical material and geometrical properties except prestressing force applied for initial stressing. The compressive strength of concrete used for casting of all plates was 40 N/mm². The impact force, deflection and failure modes of the plate specimens have been studied. It was observed that with increase in applied prestressing force impact resistance capacity of plate has been increased and magnitude of peak deflection has been reduced.

18. Ahmed Atta and Mohamed Taman, PROGRESSIVE COLLAPSE, METHODS OF PREVENTION, Saimaa University of Applied Sciences (2013)

The purpose of the study was to describe the process of progressive collapse and to find more methods and approaches to design the structure for preventing from this kind of failure. And the last aim was to find Russian norms and standards and make calculations on progressive collapse of the trade center, according to them. In this way the work was commissioned by Finnmap Consulting Oy. The thesis should be interesting to design engineers working with designing the large-span structures of public use like trade centers, stadiums or sport complexes, which are going to be built in Russia. As a result, this project described and disclosed a process of progressive collapse. Finally the calculation process for preventing structure from progressive collapse was made. And further these calculations will be used for other projects as an example.

19. Tao Yang, Wanqing Chen, and Zhongqing Han, Research Article Experimental Investigation of Progressive Collapse of Prestressed Concrete Frames after the Loss of Middle Column (2020)

Accidental loads such as explosion and vehicle impact could lead to failure of one or

several load-bearing members in the structures, which is likely to trigger disproportionate progressive collapse of overall structures. Prestressed concrete (PC) frame structures are usually at great risk of collapse once load-bearing members fail, because the members in PC frame structures are usually subjected to much more load than those in common reinforced concrete (RC) frame structures. To investigate the progressive collapse behaviours of PC frame structures, five one-fourth reduced scaled frame substructures were fabricated and collapse tests were conducted on them. Influence of span-to-depth ratios of frame beams and prestress action modes on the collapse performance of PC frame structures was discussed. Experimental results indicated that PC frame substructures with different prestress action modes, including bonded prestress and unbonded prestress, presented different collapse resistance capabilities and deformability. Tensile force increment of the unbonded prestressing strands almost linearly increased with the vertical displacement of the failed middle column. Catenary action is one of the most important mechanisms in resisting structural collapse. Prestressing strands and longitudinal reinforcing bars in the frame beams benefited the formation and maintaining of catenary action. The ultimate deformability of the PC frame structures was tightly connected with the fracture of prestressing strand. In addition, a calculation method of dynamic increase factors (DIFs) suitable for PC frame structures was developed, which can be used to revise the design collapse load when static collapse analysis is conducted by the alternative path method. The DIFs of the five substructures were discussed on the basis of the proposed method; it revealed that the DIFs corresponding to the first peak loads and the ultimate failure loads for the PC frame substructures were less than 1.49 and 1.83, respectively.

20. Qian Kai, Feng Fu, Progressive Collapse Resistance of Precast Concrete Beam-Column Subassemblages with High-Performance Dry Connections (2019)

Due to its relatively lower integrity, precast concrete structures are considered to be more vulnerable to progressive collapse than cast-in-place concrete structures. However, to date, majority of existing studies on progressive collapse focused on cast-in-place concrete structures, little attentions were paid to precast concrete structures. Among existing precast concrete structures, unbonded post-tensioning precast concrete structure is one of innovation dry connection

structural systems, which no casting at the connections on site. Its excellent seismic performance was recognized by many studies, while studies on its progressive collapse resistance were very few. To fill this knowledge gaps, in this paper, eight half-scaled unbonded post-tensioning precast concrete beam-column sub-assemblages with different connection configurations were tested through pushdown tests to investigate their capacities and resistance mechanisms to prevent progressive collapse. The test results demonstrated various behaviors of beam-column sub-assemblages with different connection types. It was found that, as the longitudinal reinforcements were discontinuous across the beam-column joint region in the beams, flexural action observed in the cast-in-place concrete frames was not mobilized for the specimens with purely unbonded post-tensioning connections. When the specimens installed top-seat angles at the beam-column interfaces, considerable flexural action capacity could be mobilized for load resistance. Moreover, it was found that the failure modes of the specimens are distinctly different to that of conventional reinforced concrete frames or precast concrete frames with cast-in-place joints. The characteristic of compressive arch action and tensile catenary action in tested specimens is quite different to that of conventional reinforced concrete frames.

21. Hou Jian, Ph.D.; Song Li, Ph.D.; and Liu Huanhuan, Testing and Analysis on Progressive Collapse-Resistance Behavior of RC Frame Substructures under a Side Column Removal Scenario (2016)

This paper presents an experimental and analytical progressive collapse-resistance evaluation of reinforced concrete (RC) frame substructures under monotonic vertical displacement of a side column, simulating a column removal scenario. A two-span, two-bay, and single-story one-third scale model representing a segment of a larger space frame structure was tested. The downward displacements of the top of the removed side column are imposed until failure. Frame collapse is defined herein as the rupture of tension steel bars in the floor beams. The study provides insight into the behavior and failure modes of the frame structure under a side column loss, including the development of catenary action in the beams and tensile membrane action in the slabs. Based on the experimental observations and theoretical analysis, a simplified calculation model of progressive collapse-resistance capacity of RC frame substructures due to the loss of a side column is established, which establishes the foundation for

progressive collapse assessment of RC frame structures. The reliability of the proposed model is verified by experimental results.

22. S. M. Marjanishvili, P.E., M. ASCE, Progressive Analysis Procedure for Progressive Collapse

Following the collapse of the World Trade Center towers in September 2001, there has been heightened interest among building owners and government entities in evaluating the progressive collapse potential of existing buildings and in designing new buildings to resist this type of collapse. The General Services Administration and Department of Defense have issued general guidelines for evaluating a building's progressive collapse potential. However, little detailed information is available to enable engineers to confidently perform a systematic progressive collapse analysis satisfying these guidelines. In this paper, we present four successively more sophisticated analysis procedures for evaluating the progressive collapse hazard: linear-elastic static; nonlinear static; linear-elastic dynamic; and nonlinear dynamic. We discuss the advantages and disadvantages of each method. We conclude that the most effective analysis procedure for progressive collapse evaluation incorporates the advantageous parts of all four procedures by systematically applying increasingly comprehensive analysis procedures to confirm that the possibility of progressive collapse is high.

23. John Abruzzo; Alain Matta, Ph.D.; and Gary Panariello, Ph.D, Study of Mitigation Strategies for Progressive Collapse of a Reinforced Concrete Commercial Building

This paper describes progressive collapse assessment of an existing reinforced concrete commercial building. Prescriptive guidelines available to date are evaluated in light of alternate load path predictions. The building, exceedingly meeting ACI integrity requirements and the recent United Facilities Criteria tie force provisions, is still significantly vulnerable to progressive collapse triggered by the loss of an interior column.

24. Jun Yu, Kang-Hai Tan, Special Detailing Techniques to Improve Structural Resistance against Progressive Collapse (2014)

Previous research work has found that catenary action can significantly increase structural resistance in addition to flexural capacity under column removal scenarios. However, whether reinforcements in beams can effectively function as ties to develop catenary action against progressive

collapse is a big concern in current engineering practice because of the limited rotational capacity of RC beam-column connections. Therefore, four RC frame specimens were designed and tested to investigate their structural behavior under a column removal scenario. In addition to a specimen designed with conventional detailing in accordance with ACI 318-05, the other three specimens were designed with special detailing techniques at little or no additional cost, endeavoring to improve catenary action capacity at large deformations without reducing the structural resistance at small deformations. The special detailing included placing an additional reinforcement layer at the midheight of beam sections, partially debonding bottom reinforcing bars in the joint region, and setting partial hinges at one beam depth away from the adjacent joint interfaces. Furthermore, the nonlinear static responses obtained from the tests were used to evaluate the progressive collapse resistances of the four specimens with the consideration of dynamic effect. With systematic instrumentation, the effects of detailing techniques on structural behavior are demonstrated in this paper at different levels. In particular, the mechanism of each special detailing to affect beam-column connection rotations is illustrated and discussed in detail. Finally, suggestions on structural design against progressive collapse via catenary action are provided.

25. Mehrdad Sasani and Serkan Sagiroglu, Gravity Load Redistribution and Progressive Collapse Resistance of 20-Story Reinforced Concrete Structure following Loss of Interior Column (2010)

The dynamic gravity-load redistribution of Baptist Memorial Hospital in Memphis, TN, a 20-story reinforced concrete (RC) structure, is evaluated and characterized experimentally and analytically following the removal of an interior ground-floor column. The structure resisted progressive collapse with a measured maximum vertical displacement of only 9.7 mm (0.38 in.). Analytical results using the finite element method are presented, which show good agreement with the experimental data. The propagation of deformation over the height of the structure and its effects on the load redistribution are presented. The effects of the remaining and bent-out steel bars of the removed column on the response of the structure are modeled and evaluated. The response of the structure due to additional dead and live loads and with complete removal of the column (including the steel bars) is analytically evaluated.

26. Kai Qian, M.ASCE; Yun-Hao Weng; and Bing Li, M.ASCE, Improving Behavior of Reinforced Concrete Frames to Resist Progressive Collapse through Steel Bracings

External installation of steel braces has been proved an effective seismic strengthening or retrofitting scheme to upgrade the lateral load-resisting capacity of reinforced concrete (RC) frames. However, the effectiveness of steel bracing in improving the progressive collapse resistance potential of RC frames is vague. To fill the gap, five one-quarter-scaled specimens (one bare frame and four braced frames) were tested subject to a pushdown loading regime. The RC frames were nonseismically detailed for reference. Four braced frames with different bracing configurations were tested to evaluate the efficiency of braces for upgrading the load-resisting capacity of RC frames. A rational design method was implemented for designing the braced frames, including the connections between the braces and RC frames. Experimental results proved that steel bracing could increase the first peak load and initial stiffness of the frames significantly. Before mobilization of catenary action in RC frames, the tensile braces were fractured, but the compressive braces experienced severe buckling. Consequently, the braced specimens performed similarly to the bare frame in the catenary action stage.

27. Rohit B. Nimse, Digesh D. Joshi, Paresh V. Patel Behavior of wet precast beam column connections under progressive collapse scenario: an experimental study

Progressive collapse denotes a failure of a major portion of a structure that has been initiated by failure of a relatively small part of the structure such as failure of any vertical load carrying element (typically columns). Failure of large part of any structure will result into substantial loss of human lives and natural resources. Therefore, it is important to prevent progressive collapse which is also known as disproportionate collapse. Nowadays, there is an increasing trend toward construction of buildings using precast concrete. In precast concrete construction, all the components of structures are produced in controlled environment and they are being transported to the site. At site such individual components are connected appropriately. Connections are the most critical elements of any precast structure, because in past major collapse of precast structure took place because of connection failure. In this study, behavior of three different 1/3rd scaled wet precast beam column connections under progressive collapse scenario are studied and its performance is

compared with monolithic connection. Precast connections are constructed by adopting different connection detailing at the junction by considering reinforced concrete corbel for two specimens and steel billet for one specimen. Performance of specimen is evaluated on the basis of ultimate load carrying capacity, maximum deflection and deflection measured along the span of the beam. From the results, it is observed that load carrying capacity and ductility of precast connections considered in this study are more than that of monolithic connections.

28. Kai, Qian; Li, Bing Slab effects on response of reinforced concrete substructures after loss of corner column (2012)

In typical cast-in-place construction, beams, columns, and slabs act as a single structural unit. Ignoring the slab contribution to the strength and ductility of beams will result in a significant underestimation of the vertical force resistance. The influence of the slab on the strength of the floor system under imposed vertical deformation is significantly greater than that anticipated by the interpretation of the current provisions for effective slab widths acting as a flange in a T-beam analysis. Therefore, to quantify the contribution of the slab toward progressive collapse of building structures in the blast environment, two series of specimens (F and S) were tested under monotonic loading to simulate axial loading in the corner column. The experimental results highlighting the behaviour, such as force displacement responses, crack patterns, and failure mechanisms, were discussed. Comparison of the performance of these two series of specimens indicated that incorporating the reinforced concrete (RC) slab into the beam-column substructures would increase the ultimate resistance capacity by up to 63.0% and significantly reduce the likelihood of progressive collapse.

29. Qian, Kai; Li, Bing, Investigation into resilience of precast concrete floors against progressive collapse (2019)

The casualties and economic loss in historic events have revealed that progressive collapse performance of buildings has to be evaluated in structural design to prevent such disastrous events. Integrity and resilience are important characteristics for buildings to prevent total collapse or disproportionate collapse once an unpredictable terrorism event unfortunately occurs. Compared to the extensive studies on behavior of cast-in-place reinforced concrete (RC) buildings for progressive collapse resistance, there is less

research on precast concrete (PC) buildings to mitigate progressive collapse. Thus, in this study, three one-story, two-bay largescale frame-floor subassemblies (one RC and two PC) are tested under pushdown loading regime to investigate the effect of PC floor units and transverse beams on progressive collapse resilience of PC moment-resisting frames. It is found that the PC beams and slab systems could provide substantial compressive arch action and compressive membrane action, similar to the cast-in-place RC buildings. However, as PC slabs are discontinuous, insignificant tensile membrane action is able to develop in PC slab systems and the ultimate load capacity in enormous deformation stage is mainly attributed to the catenary action developed in PC beams.

30. JianwuPan , Xian Wang , and Fang Wu, Strengthening of Precast RC Frame to Mitigate Progressive Collapse by Externally Bonded CFRP Sheets Anchored with HFRP Anchors (2018)

Currently, the robustness of precast reinforced concrete frames is attracting wide attention. However, avoiding “strong beams and weak columns” during strengthening against progressive collapse is a key problem. To discuss this problem, an experimental study on two 1/2-scale precast frame sub assemblages under a pushdown loading regime was carried out in this paper. One specimen was strengthened with carbon fibre-reinforced polymer (CFRP) sheets on the beam sides. The middle parts of the CFRP sheets were anchored with hybrid fibre-reinforced polymer (HFRP) anchors. Another specimen was not strengthened. The failure mechanisms, failure modes, and strengthening effect are discussed. The strengthening effect is very obvious in the early catenary action stage. No shearing failure develops on HFRP anchors, which proves that the anchoring method is effective. Based on the experimental results, analytical models and preventive strengthening design and construction measures to mitigate progressive collapse of the precast RC frame are proposed.

31. Spencer E. Quiel, Clay J. Naito, Corey T. Fallon A non-emulative moment connection

for progressive collapse resistance in precast concrete building frames (2019)

This paper documents the experimental development of a new spandrel-to-column moment connection detail for progressive collapse resistance in precast concrete building frames. This study focuses on a 10-story prototype precast concrete frame building with perimeter special moment frames (SMF) that are subjected to a ground floor column removal. The experimental subassembly represents a spandrel-to-column connection on the perimeter SMF near the middle of the building face (i.e. not at the corners). The connection is non-emulative and utilizes unbonded high-strength steel post-tensioning (PT) bars which pass through ducts in the column and are anchored to the spandrels via bearing plates. The proposed design strives for construction simplicity, avoids field welding and/or grouting, and maximizes ductility by allowing the high strength steel bars to act as structural “fuses” when yielding. A full-scale quasi-static pushdown test is performed on two variants of the proposed connection: one with higher moment-rotation capacity and limited ductility, and another with lower capacity and higher ductility. The results show that the connection can reliably achieve its design yield capacity, performs well under service level demands, and can achieve moderate-to-high ductility. The experimental results are then applied to a system-level computational model of the prototype building frame under a column removal scenario. The results of a nonlinear dynamic analysis demonstrate that the system can arrest progressive collapse in the event of a single column loss scenario when either variant of the proposed connection is considered.

III. MODEL AND ANALYSIS

1.2 Modeling on ANSYS

In order to calculate the desired blast intensity 3D ANSYS model was prepared and analysis was performed for 100 kg TNT Blast at 5m distance from the building. The shock waves created due to the blast will result in deformation of the building. This shock waves transmitted to the building with respect to the time in second was calculated with this analysis. The Fig. 3.1 shows the pressure (MPa) with respect to the time.

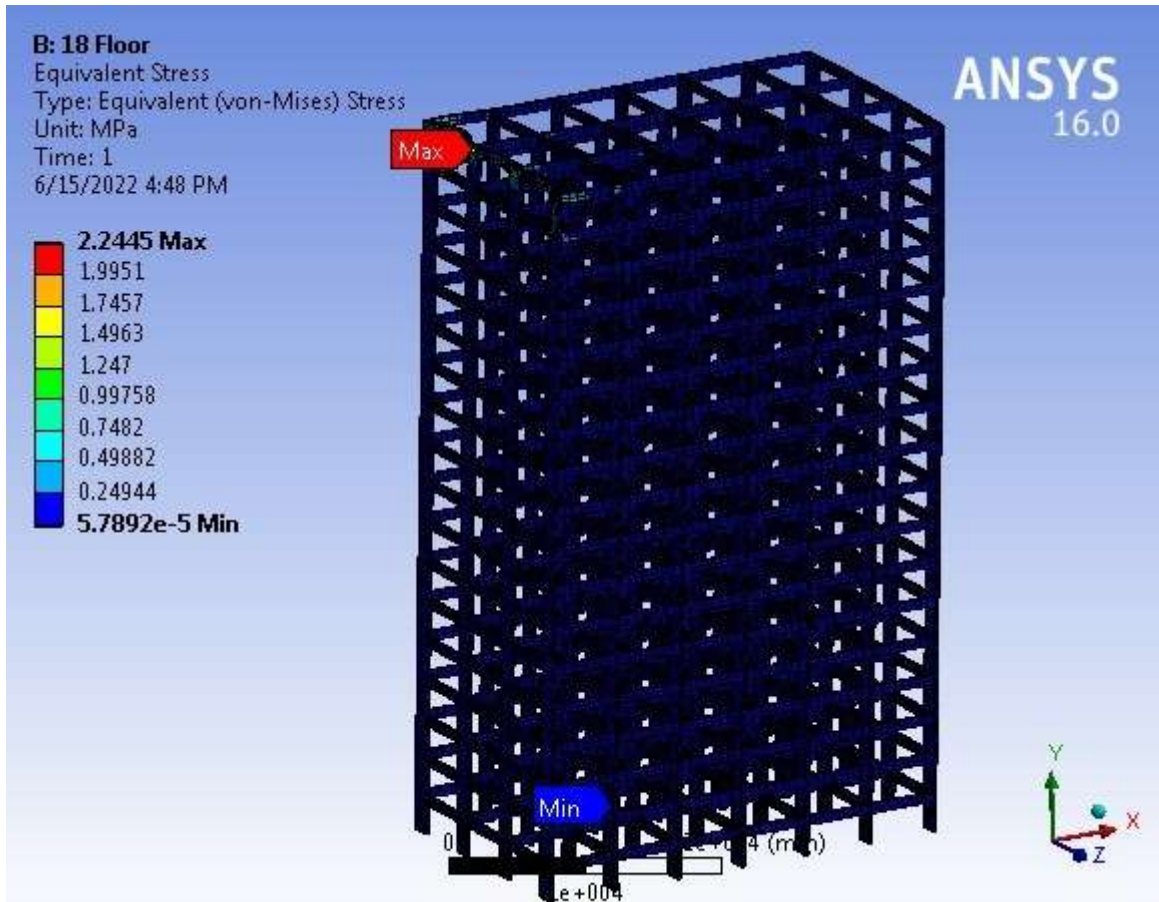


Fig. 3.1 Pressure (MPa) with respect to the time for G+18

3.1.1 Properties Assigned to the Model

A) Material Properties

1. Young's Modulus: 27386.12 Mpa
2. Poisson's Ratio: 0.2
3. Coefficient of Thermal Expansion: 0.0000099
4. Compressive Strength: 30MPa

B) Model Properties

1. Floor to Floor Height: 3m
2. Number of Floors: 18
3. Height of Building: 54m

3.1.2 Time v/s Pressure Results

Table No.3.1 Time v/s Pressure Results

TIME (in Sec)	VALUE (in MPa)
0.3	2.355
0.6	2.090
0.9	1.830
1.0	1.570
1.2	1.300

1.5	0.780
1.8	0.260

1.3 Time-History Analysis

3.2.1 Definition

Time history analysis is a step-by- step analysis of the dynamic response of a structure to a specified loading that may vary with time. Time history analysis is used to determine the seismic response of a structure under dynamic loading of representative earthquake.

In this study use of time history analysis is done to analyse the effect of blast on high rise buildings using FEM based software ETABS. The graph of Pressure v/s Time obtained from the ANSYS analysis will be used as input values for Time-History analysis.



Graph No. 01: Graph showing Pressure v/s Time

1.4 Etabs Model Inputs in Pre-Analysis

3.3.1 Data Sheet

1. Type of Building: Residential Building
2. Number of Floors: Basement + Podium + 1 to 15 Floors + Terrace + OHWT
3. Floor to Floor Height: 3m
4. Slab Thickness: 150mm
5. Grade of Concrete: M40/M35
6. Type of Cladding: Light weight Blocks (9 KN/m³ with mortar)
7. Live Load (Parking): 4KN/m²
8. Live Load (Typical Floor): 2KN/m²
9. Floor Finish (Parking): 2KN/m²
10. Floor Finish (Typical Floor): 1.5 KN/m²
11. Sunk Load: 4KN/m²
12. Wall Load = (3-0.6) X 0.15 X 9 = 3.2 KN/Rm
13. Wall Thickness: 150mm

14. Beam Size: 230 X 600mm
15. Shear wall: 300/230 mm thk

3.3.2 Design IS Codes

1. IS 456:2000
2. IS 875 Part 1 to 5
3. IS 1893:2016
4. IS 16700:2017

3.3.3 Details of Model

A) Static Analysis

1. Location of Building: Mumbai
2. Seismic Zone: III
3. Zone factor: 0.16
4. Importance Factor: 1.2
5. Response Reduction: 4
6. Time Period: As per Tax & Tay = 0.075 X H/Sqrt AW

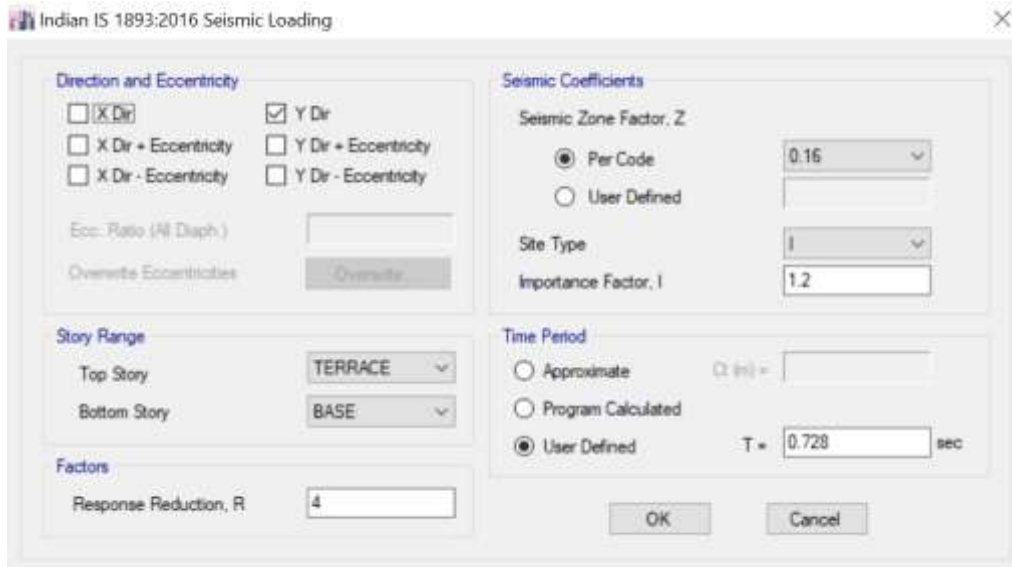


Fig. 3.2 Seismic Coefficient in X Direction

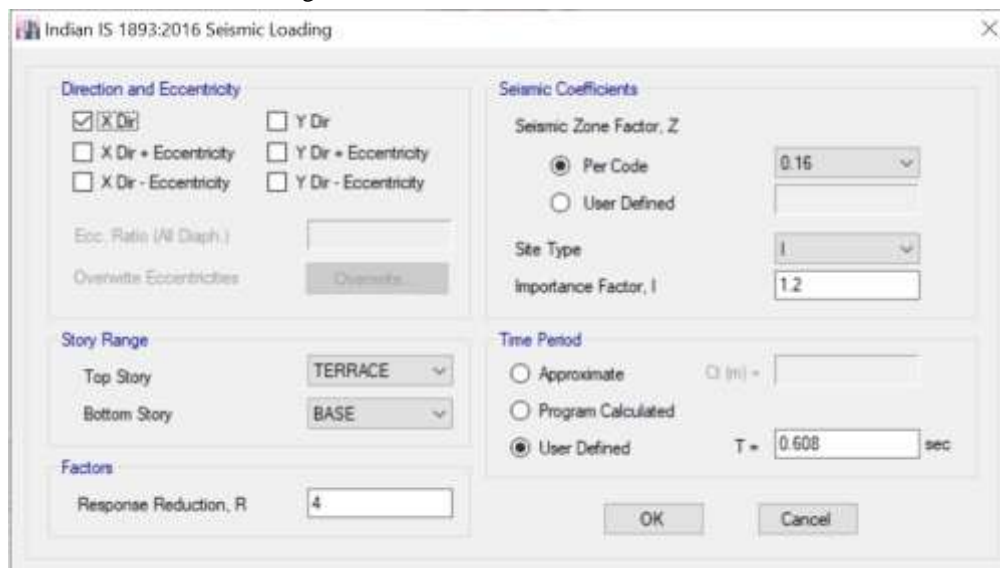


Fig. 3.3 Seismic Coefficient in Y Direction

B) Dynamic Analysis (Time-History Analysis)
 Acceleration Spectrum: 9810 mm²/Sec

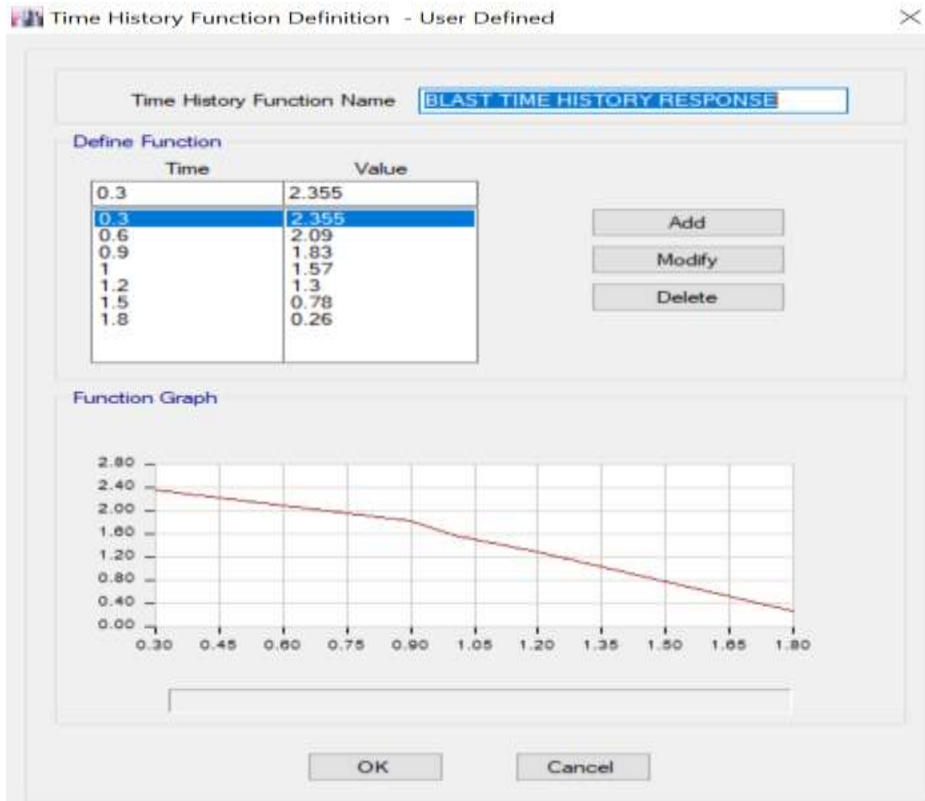


Fig. 3.4 Time History Function

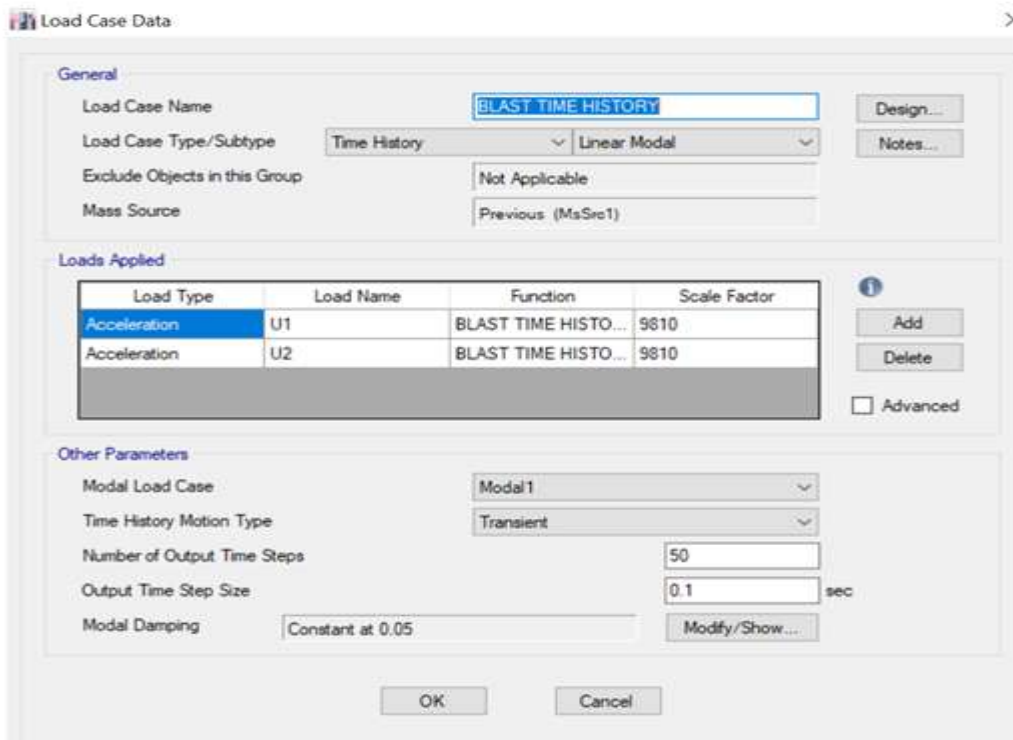


Fig. 3.5 Time History Load Case

C) Wind Analysis

1. Location: Mumbai
2. Basic Wind speed: $V_b = 44$ m/sec
3. Terrain Category: III
4. Importance Factor: 1
5. Risk Coefficient (K1): 1
6. Topography Factor (K3): 1

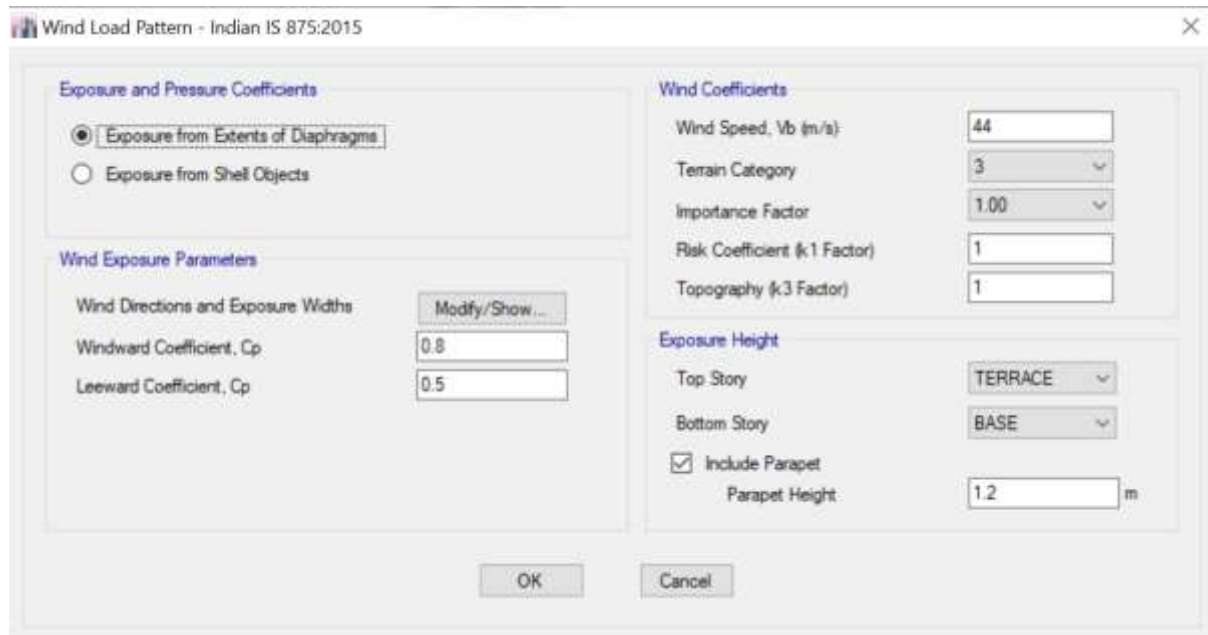


Fig.3.6 Design Wind Speed Pressure in X and Y direction

D) Load Combination

- | | | |
|--|--|--|
| 1) DL+LL | | 14) 1.2DL + 1.2LL+1.2SP Y |
| 2) 1.5(DL+LL) | | 15) 1.2DL+1.2LL-1.2EQY |
| 3) 1.5(DL+EQY) | | 16) 1.2(DL+LL+WX) |
| 4) 1.5(DL-EQY) | | 17) 1.2(DL+LL+GX) |
| 5) 1.5(DL+WX) | | 18) 0.9DL+1.5WX |
| 6) 1.5(DL + GX) | | 19) 0.9DL-1.5WX |
| 7) 1.5(DL - WX) | | 20) 0.9DL+1.5WY |
| 8) 1.5(DL - GX) 9) 1.5(DL + WY) | | 21) 0.9DL+1.5GY |
| 9) 1.5(DL + GY) 10) 1.5(DL - WY) | | 22) 0.9DL-1.5WY |
| 10) 1.5(DL - GY) | | Time-History and Wind Combination |
| 11) 1.2DL+1.2LL+1.2EQX | | 1) 0.9DL-1.5WLX TH |
| 12) 1.2DL+1.2LL-1.2EQX | | 2) 0.9DL-1.5WLY+TH |
| 13) 1.2DL+1.2LL-1.2SPEC X 13) 1.2DL+1.2LL+1.2EQY | | 3) 0.9DL+1.5WLX+TH |
| | | 4) 0.9DL+1.5WLY+TH |

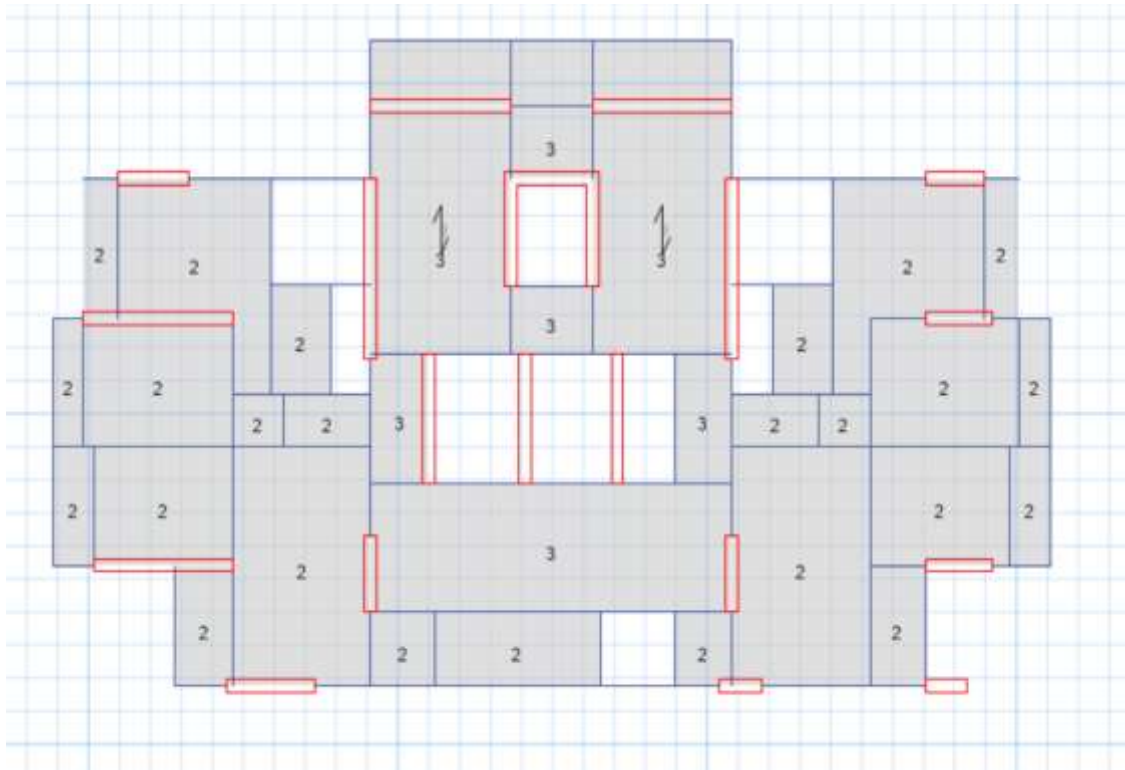


Fig.3.7 Live load on Typical floor

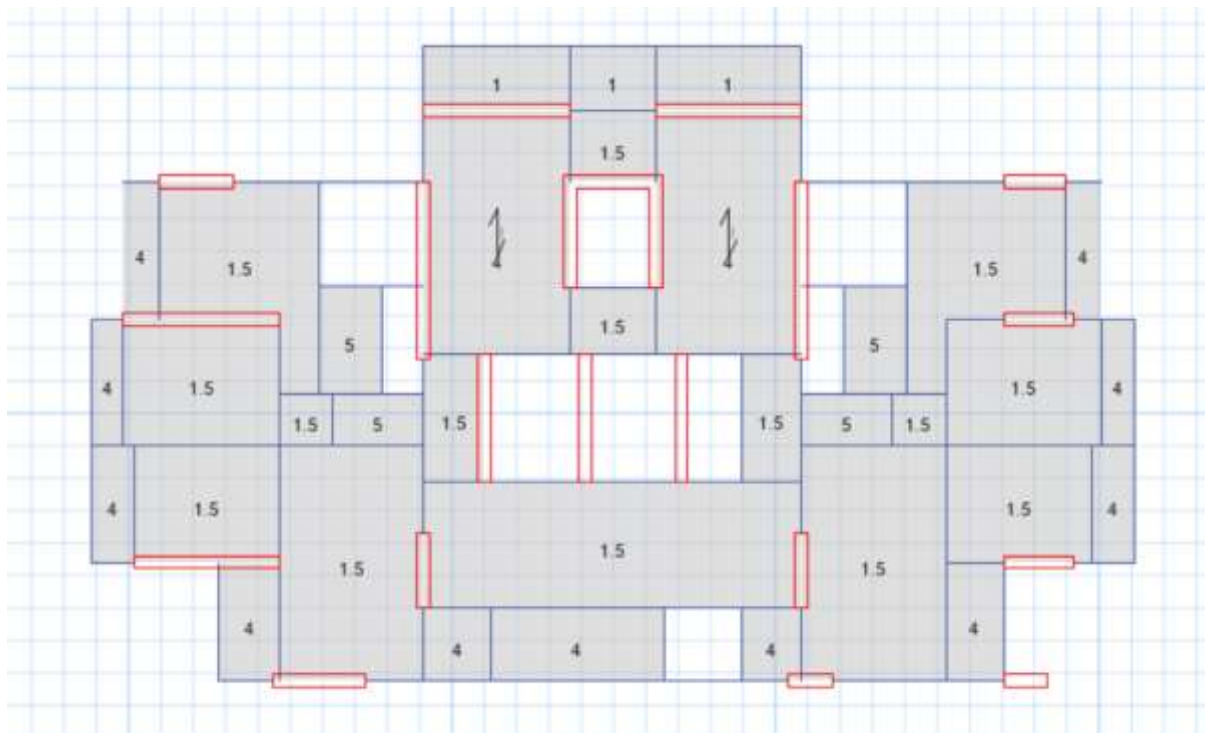


Fig.3.8 SDL (Floor finish and Sunk load) on typical floor

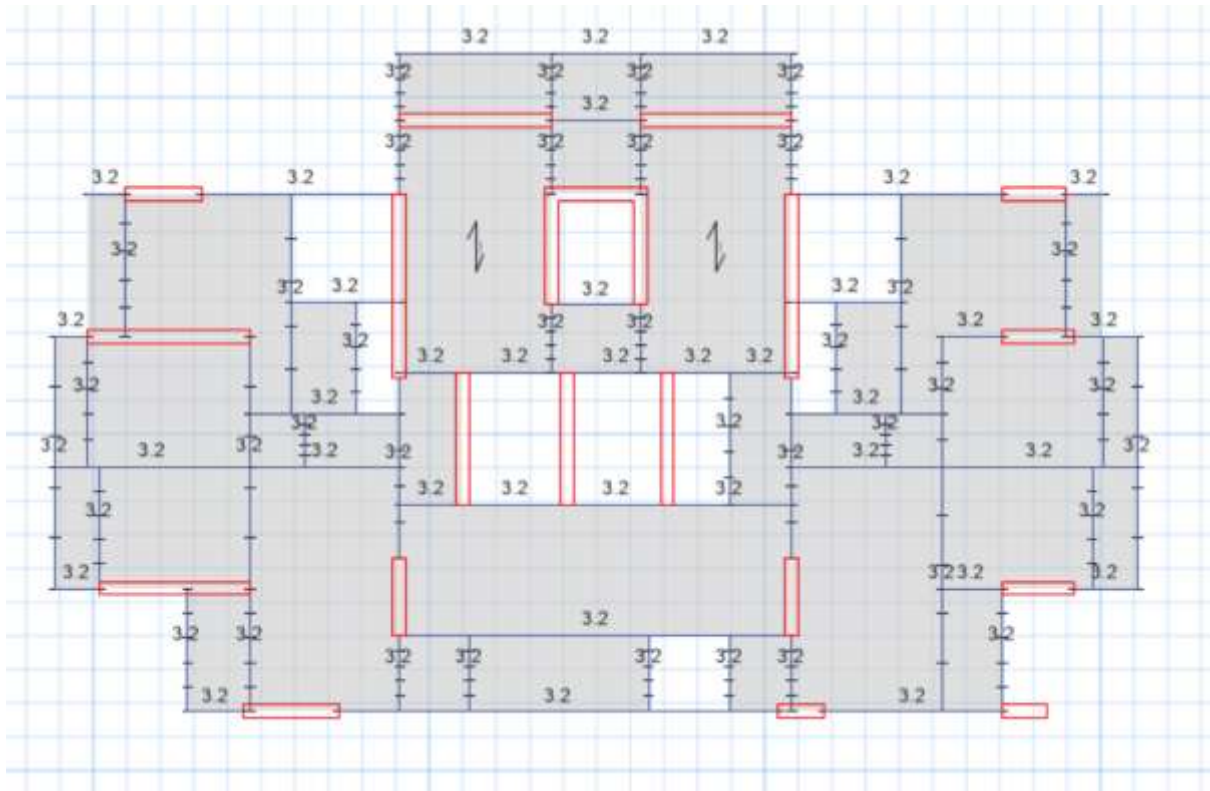


Fig.3.9 Wall Load on Typical Floor

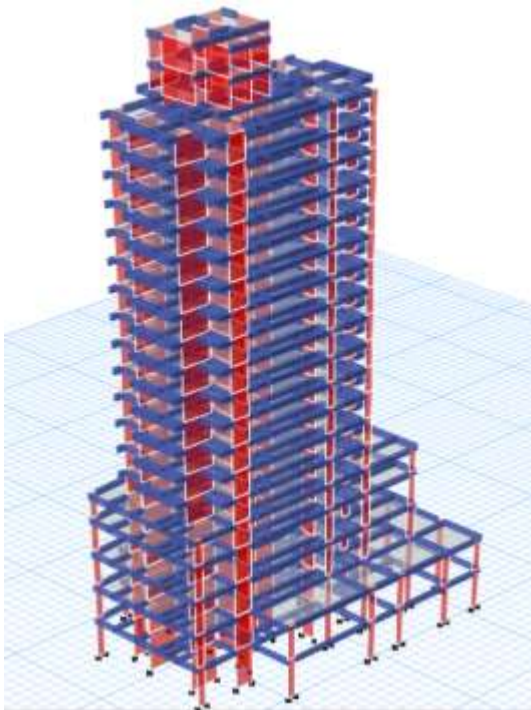


Fig.3.10 G +15 Model

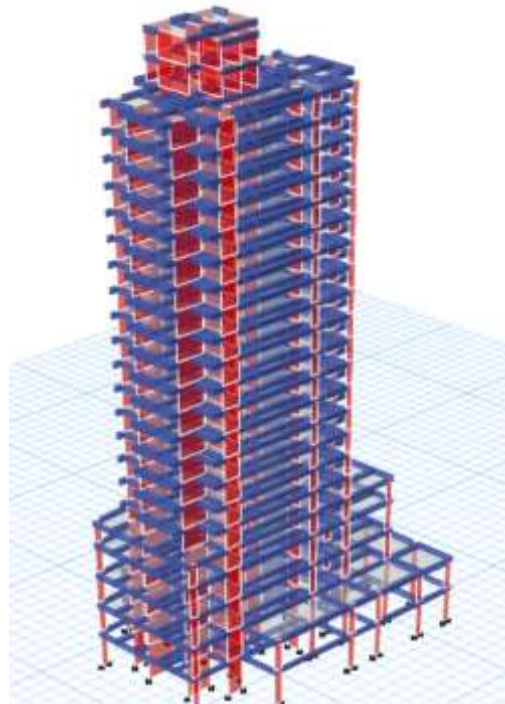


Fig.3.11 G +18 Model

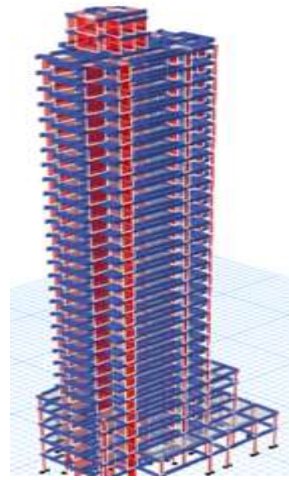


Fig.3.12 G +24 Model

1.5 Etabs Model - Post-Analysis (G+24)

3.4.1 Mass Participation

The Mass participation factor is a mass percentage factor that represents how much of the structure

participates in the vibration for each vibration mode when the structure is vibrated at a complex vibration mode.

Table No.3.2 Result showing Mass Participation, Time Period and Torsion (G+24)

Mode	Period sec	UX	UY	U Z	Sum UX	Sum UY	Sum UZ	RX	RY	RZ	Sum RX	Sum RY	Sum RZ
1	4.243	0.4846	0.0033	0	0.4846	0.0033	0	0.0017	0.2384	0.1559	0.0017	0.2384	0.1559
2	3.693	0.0092	0.6453	0	0.4938	0.6486	0	0.3419	0.0041	0.0004	0.3435	0.2425	0.1563
3	2.65	0.1684	0.0069	0	0.6622	0.6556	0	0.0045	0.0988	0.4265	0.3475	0.3411	0.5832
4	1.247	0.1054	0.0027	0	0.7675	0.6583	0	0.0023	0.1866	0.0403	0.3498	0.5277	0.6235
5	0.995	0.0037	0.1769	0	0.7712	0.8353	0	0.3029	0.0066	4.46E-05	0.6526	0.5343	0.6236
6	0.833	0.0431	0.0005	0	0.8143	0.8358	0	0.0019	0.0956	0.1229	0.6546	0.6299	0.7465
7	0.663	0.0457	0.0036	0	0.864	0.8394	0	0.0055	0.0712	0.0283	0.661	0.7011	0.7748
8	0.487	0.0075	0.0493	0	0.8674	0.8887	0	0.0865	0.0107	0.0246	0.7465	0.7118	0.7994
9	0.469	0.0037	0.0103	0	0.8711	0.899	0	0.0174	0.0038	0.0563	0.7646	0.7156	0.8557
10	0.42	0.0379	0.002	0	0.9091	0.901	0	0.0037	0.069	0.0014	0.7676	0.7846	0.8571
11	0.317	0.0018	0.0106	0	0.9108	0.9117	0	0.0233	0.0046	0.0285	0.7909	0.7892	0.8856
12	0.298	0.0008	0.0184	0	0.9116	0.9301	0	0.0414	0.0016	0.0039	0.8322	0.7908	0.8895
13	0.284	0.0239	0.0022	0	0.9355	0.9323	0	0.0051	0.0534	4.22E-05	0.8373	0.8442	0.8896
14	0.211	0.0019	0.0177	0	0.9373	0.95	0	0.0392	0.004	0.0094	0.8765	0.8482	0.8989
15	0.193	0.0201	0.0031	0	0.9574	0.9531	0	0.0069	0.0445	0.001	0.8834	0.8927	0.9
16	0.145	0.0045	0.018	0	0.9619	0.971	0	0.0426	0.0108	0.0005	0.926	0.9035	0.9005
17	0.108	0.0223	0.0053	0	0.9839	0.9763	0	0.0135	0.0545	0.006	0.939	0.958	0.9065
18	0.083	0.0031	0.0125	0	0.987	0.9887	0	0.0312	0.0075	0.0006	0.9702	0.9655	0.9071

3.4.2 Joint Displacement at Terrace

Lateral displacement is important when structures are subjected to lateral loads like earthquake and wind loads. Lateral displacement depends on height of structure and slenderness of the structure because structures are more vulnerable as height of

building increases by becoming more flexible to lateral loads.

Allowable displacement as per IS 16700

A) For Earthquake – $H/250=324\text{mm}$

B) For Wind – $H/500=206\text{mm}$

Where H = Total height of Building above ground

Table No. 3.3 Joint Displacement at Terrace for Combination 0.9DL+1.5WY (G+24)

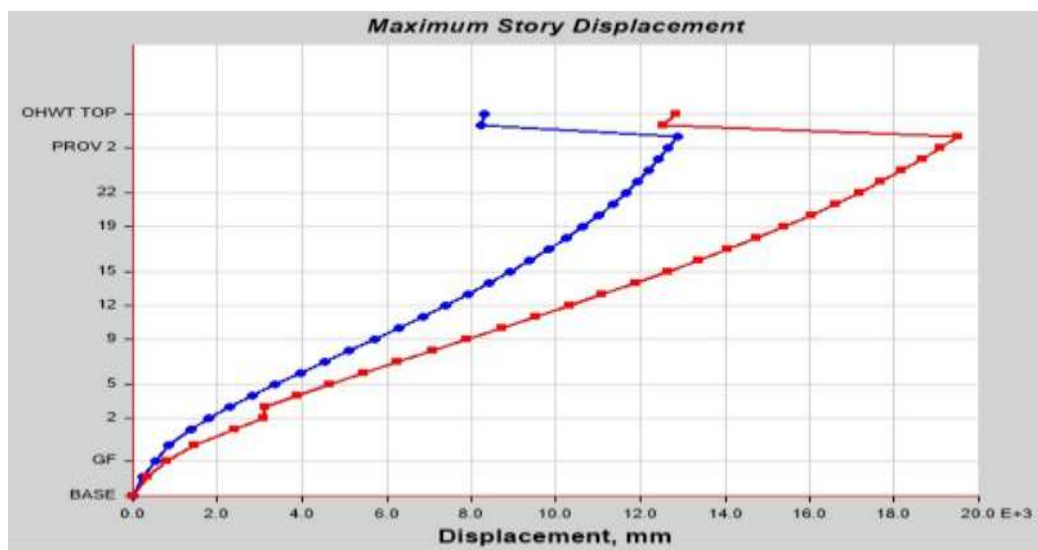
TABLE: Joint Displacements									
Story	Label	Unique Name	Load Case/Combo	UX	UY	UZ	RX	RY	RZ
				mm	mm	mm	rad	rad	rad
TERRACE	14	98	21) 0.9DL+1.5WY	204.247	73.193	-12.229	0.000315	0.001403	0.005382
TERRACE	26	3424	21) 0.9DL+1.5WY	204.17	23.417	-25.469	0.00053	0.001439	0.005267
TERRACE	136	91	21) 0.9DL+1.5WY	142.192	25.811	-23.138	0.001259	0.00125	0.005404
TERRACE	125	171	21) 0.9DL+1.5WY	142.168	-87.38	-4.157	0.001218	0.001175	0.005374

Table No. 3.4 Joint Displacement at Terrace for Combination 0.9DL+1.5WLX+TH Max(G+24)

TABLE: Joint Displacements									
Story	Label	Unique Name	Load Case/Combo	UX	UY	UZ	RX	RY	RZ
				mm	mm	mm	rad	rad	rad
TERRACE	26	3424	0.9DL+1.5WLX+T H Max	13247.78	17652.98	135.33	0.178647	0.070545	1.032509
TERRACE	14	98	0.9DL+1.5WLX+T H Max	13245.53	6549.37	372.722	0.125684	0.072418	1.039656
TERRACE	26	3424	0.9DL+1.5WLY+T H Max	13058.58	17833.75	149.532	0.176644	0.069261	1.027548
TERRACE	26	3424	0.9DL+1.5WLY+TH Max	13056.45	17355.53	132.127	0.181257	0.069294	1.025814

Graph No. 2 Displacement v/s Storey(G+24)

3.4.3 Drift



Storey drift is the lateral displacement of a floor relative to the floor below, and the storey drift ratio is the storey drift divided by the storey height.

Allowable drift as per IS 16700 = 0.0004 X hi

Where hi=Storey height

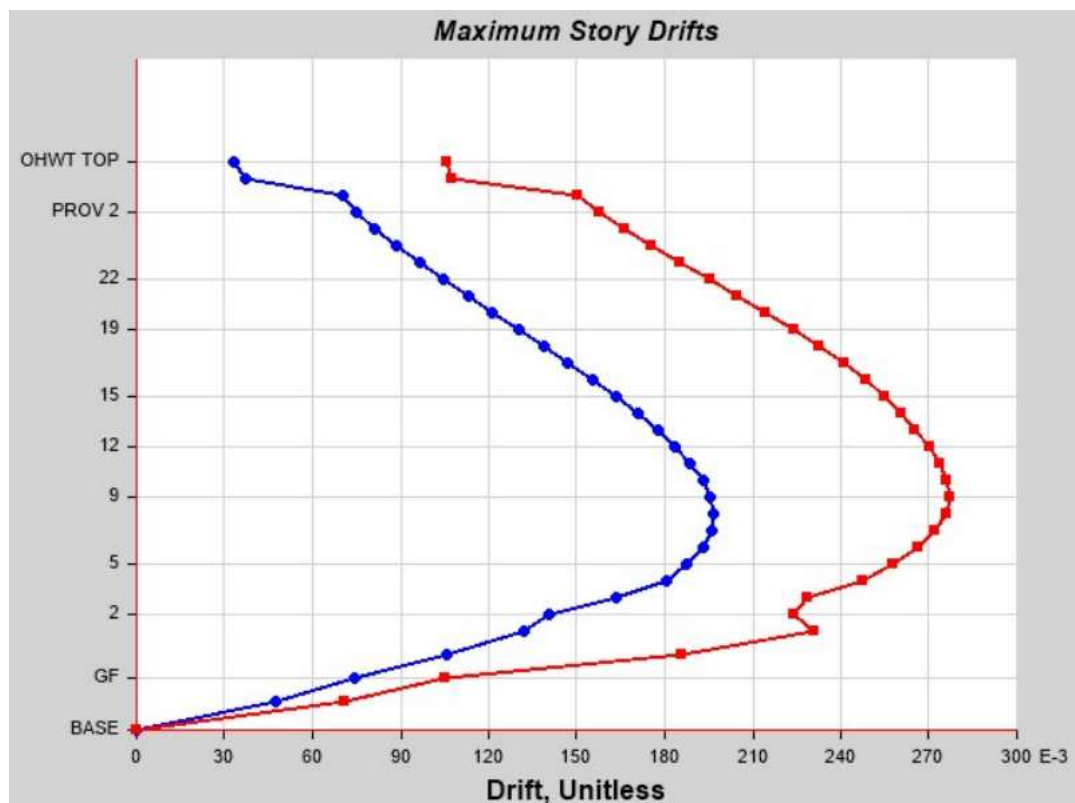
Table No. 3.5 Storey Drift for 1.5(DL-WY) combination(G+24)

TABLE: Story Drifts				
Story	Load Case/Combo	Direction	Drift	Label
14	10) 1.5(DL-WY)	Y	0.003843	46

Table No. 3.6 Storey Drift for 0.9DL-1.5WLY+TH Min combination(G+24)

TABLE: Story Drifts				
Story	Load Case/Combo	Direction	Drift	Label
9	0.9DL-1.5WLY+TH Min	Y	0.309367	46

Graph No. 3Drift v/s Storey(G+24)



3.5 Etabs Model - Post-Analysis (G+18)

3.5.1 Mass Participation

Table No.3.7 Result showing Mass Participation, Time Period and Torsion (G+18)

Mode	Period sec	UX	UY	UZ	Sum UX	Sum UY	Sum UZ	RX	RY	RZ	Sum RX	Sum RY	Sum RZ
1	4.243	0.4846	0.0033	0	0.4846	0.0033	0	0.0017	0.2384	0.1559	0.0017	0.2384	0.1559
2	3.693	0.0092	0.6453	0	0.4938	0.6486	0	0.3419	0.0041	0.0004	0.3435	0.2425	0.1563
3	2.65	0.1684	0.0069	0	0.6622	0.6556	0	0.004	0.0985	0.4268	0.3475	0.3411	0.5832
4	1.247	0.1054	0.0027	0	0.7675	0.6583	0	0.0023	0.1866	0.0403	0.3498	0.5277	0.6235
5	0.995	0.0037	0.1769	0	0.7712	0.8353	0	0.3029	0.0066	4.46E-05	0.6526	0.5343	0.6236
6	0.833	0.0431	0.0005	0	0.8143	0.8358	0	0.0019	0.0956	0.1229	0.6546	0.6299	0.7465
7	0.663	0.0457	0.0036	0	0.86	0.8394	0	0.0055	0.0712	0.0283	0.66	0.7011	0.7748
8	0.487	0.0075	0.0493	0	0.8674	0.8887	0	0.0865	0.0107	0.0246	0.7465	0.7118	0.7994
9	0.469	0.0037	0.0103	0	0.8711	0.899	0	0.0174	0.0038	0.0563	0.764	0.7156	0.8557
10	0.42	0.0379	0.002	0	0.909	0.9011	0	0.0037	0.069	0.0014	0.7676	0.7846	0.8571
11	0.317	0.0018	0.0106	0	0.9108	0.9117	0	0.0233	0.0046	0.0285	0.7909	0.7892	0.8856
12	0.298	0.0008	0.0184	0	0.9116	0.9301	0	0.0414	0.0016	0.0039	0.8322	0.7908	0.8895
13	0.284	0.0239	0.0022	0	0.9355	0.9323	0	0.0051	0.0534	4.22E-05	0.8373	0.8442	0.8896
14	0.211	0.0019	0.0177	0	0.9373	0.95	0	0.0392	0.004	0.0094	0.8765	0.8482	0.8989
15	0.193	0.0201	0.0031	0	0.9574	0.9531	0	0.0069	0.0445	0.001	0.8834	0.8927	0.9
16	0.145	0.0045	0.018	0	0.9619	0.971	0	0.0426	0.0108	0.0005	0.926	0.9035	0.9005
17	0.108	0.022	0.0053	0	0.9839	0.9763	0	0.013	0.0545	0.006	0.939	0.958	0.9065
18	0.083	0.0031	0.0125	0	0.987	0.9887	0	0.0312	0.0075	0.0006	0.9702	0.9655	0.9071

3.5.2 Joint Displacement at Terrace

Allowable displacement as per IS 16700

- A) For Earthquake – $H/250=276\text{mm}$
- B) For Wind – $H/500=143\text{mm}$

Where H = Total height of Building above ground

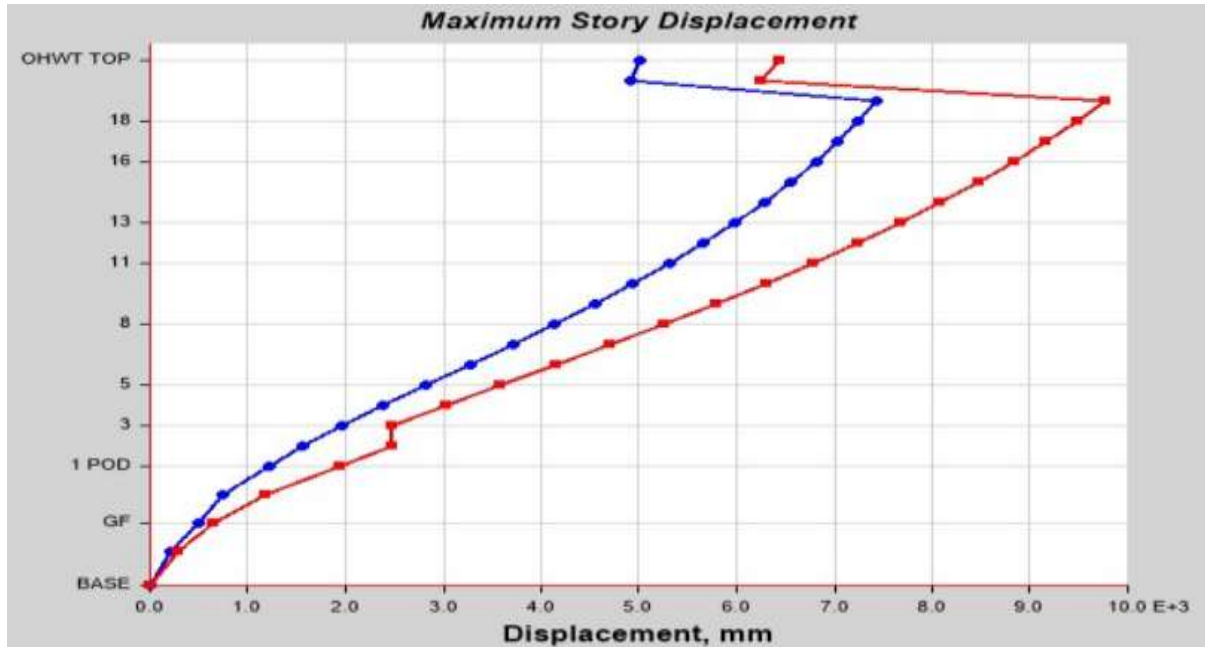
Table No. 3.8 Joint Displacement at Terrace for Combination 1.5(DL+EQX) (G+18)

TABLE: Joint Displacements									
Story	Label	Unique Name	Load Case/Combo	UX	UY	UZ	RX	RY	RZ
				mm	mm	mm	rad	rad	rad
TERRACE	15	151	3) 1.5(DL+EQX)	298.082	-91.856	-10.818	0.000066	0.003195	0.009526
TERRACE	15	151	ENV Max	298.082	135.7	-0.121	0.00193	0.003195	0.009678
TERRACE	26	3424	3) 1.5(DL+EQX)	297.917	77.967	-26.178	-0.00014	0.003289	0.009277
TERRACE	26	3424	ENV Max	297.917	153.678	-2.055	0.003141	0.003289	0.009472

Table No. 3.9 Joint Displacement at Terrace for Combination 0.9DL+1.5WLX+TH Max

TABLE: Joint Displacements									
Story	Label	Unique Name	Load Case/Combo	UX	UY	UZ	RX	RY	RZ
				mm	mm	mm	rad	rad	rad
TERRACE	26	3424	0.9DL+1.5WLX+TH Max	7589.024	8805.948	229.642	0.125481	0.064825	0.563935
TERRACE	14	98	0.9DL+1.5WLX+TH Max	7588.733	3748.944	195.506	0.080568	0.064514	0.569614
TERRACE	26	3424	0.9DL+1.5WLY+TH Max	7509.5	8871.545	234.697	0.1246	0.064084	0.561714
TERRACE	26	3424	0.9DL-1.5WLY+TH Max	7509.321	8689.636	229.003	0.126803	0.064062	0.56115

Graph No.4 Displacement v/s Storey for G+18



3.5.3 Drift

Allowable drift as per IS 16700 = 0.0004 X hi
 Where hi=Storey height

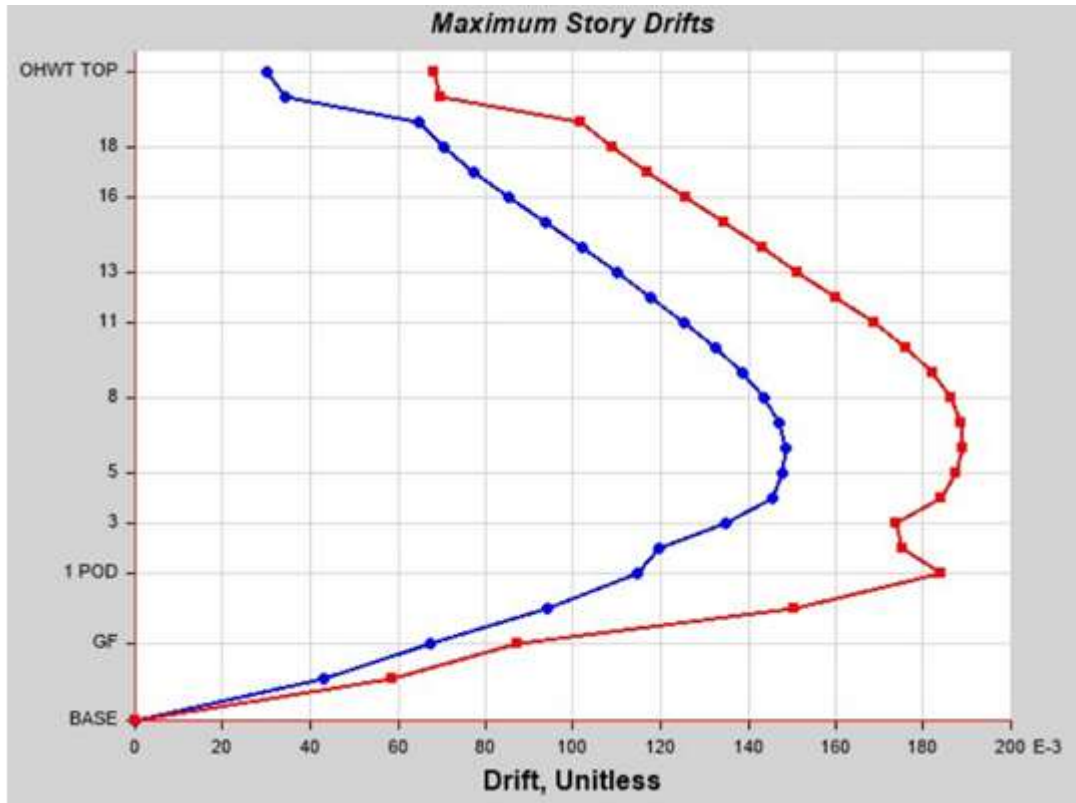
Table No. 3.10 Storey Drift for 0.9DL+1.5WLX+TH Max combination (G+18)

TABLE: Story Drifts							
Story	Load Case/Combo	Direction	Drift	Label	X	Y	Z
					m	m	m
18	0.9DL+1.5WLX+TH Max	Y	0.109169	46	117.825	107.5526	68.6

Table No. 3.11 Storey Drift for 0.9DL-1.5WLY+TH Min combination (G+18)

TABLE: Story Drifts				
Story	Load Case/Combo	Direction	Drift	Label
9	0.9DL-1.5WLY+TH Min	Y	0.0036	46

Graph No.5 Drift v/s Storey for G+18



3.6Etabs Model - Post-Analysis (G+15)

3.6.1 Mass Participation

Table No.3.12 Result showing Mass Participation, Time Period and Torsion (G+15)

TABLE: Modal Participating Mass Ratios													
Mode	Period	UX	UY	UZ	Sum UX	Sum UY	Sum UZ	RX	RY	RZ	Sum RX	Sum RY	Sum RZ
	sec												
1	2.386	0.4592	0.0012	0	0.4592	0.0012	0	0.0003	0.2302	0.1724	0.0003	0.2302	0.1724
2	1.983	0.0059	0.6654	0	0.4651	0.6665	0	0.3277	0.0023	0.0008	0.328	0.2325	0.1732
3	1.553	0.1975	0.0061	0	0.6626	0.6727	0	0.0048	0.11	0.4001	0.3328	0.3425	0.5733
4	0.74	0.1012	0.0069	0	0.7638	0.6795	0	0.0062	0.1654	0.0779	0.339	0.5079	0.6513
5	0.575	0.0118	0.1686	0	0.7756	0.8481	0	0.3345	0.0238	0.0054	0.6735	0.5317	0.6567
6	0.526	0.056	0.005	0	0.8316	0.8532	0	0.015	0.124	0.1364	0.6886	0.6558	0.7931
7	0.386	0.0405	0.0042	0	0.8721	0.8574	0	0.0073	0.0683	0.0328	0.6958	0.724	0.8259
8	0.29	0.0202	0.0187	0	0.8923	0.8761	0	0.0336	0.0293	0.0428	0.7294	0.7533	0.8687
9	0.272	0.002	0.0364	0	0.8942	0.9125	0	0.0609	0.0025	0.0139	0.7903	0.7558	0.8826
10	0.236	0.0244	0.0027	0	0.9186	0.9152	0	0.0057	0.046	0.0236	0.796	0.8018	0.9062
11	0.191	0.0052	0.0068	0	0.9238	0.922	0	0.0154	0.0123	0.0349	0.8114	0.8141	0.941
12	0.165	0.0024	0.0239	0	0.9262	0.9459	0	0.0554	0.006	0.0015	0.8668	0.8201	0.9425
13	0.163	0.0167	0.002	0	0.943	0.948	0	0.0045	0.0394	0.0026	0.8713	0.8595	0.9451
14	0.131	0.0156	0.0003	0	0.9586	0.9482	0	0.0005	0.0351	0.0061	0.8719	0.8946	0.9512
15	0.112	0.0001	0.0264	0	0.9587	0.9746	0	0.0609	0.0002	0.0011	0.9328	0.8948	0.9523
16	0.098	0.0163	8.9E-07	0	0.975	0.9746	0	4.256E-06	0.0384	0.0001	0.9328	0.9332	0.9525
17	0.052	0.0002	0.013	0	0.9752	0.9876	0	0.0341	0.0006	0.0001	0.9669	0.9338	0.9526
18	0.046	0.0142	0.0002	0	0.9895	0.9877	0	0.0004	0.0375	0.0011	0.9673	0.9713	0.9537

3.6.2 Joint Displacement at Terrace

Allowable displacement as per IS 16700

A) For Earthquake – $H/250=248\text{mm}$

B) For Wind – $H/500 =124\text{mm}$

Where H = Total height of Building above ground

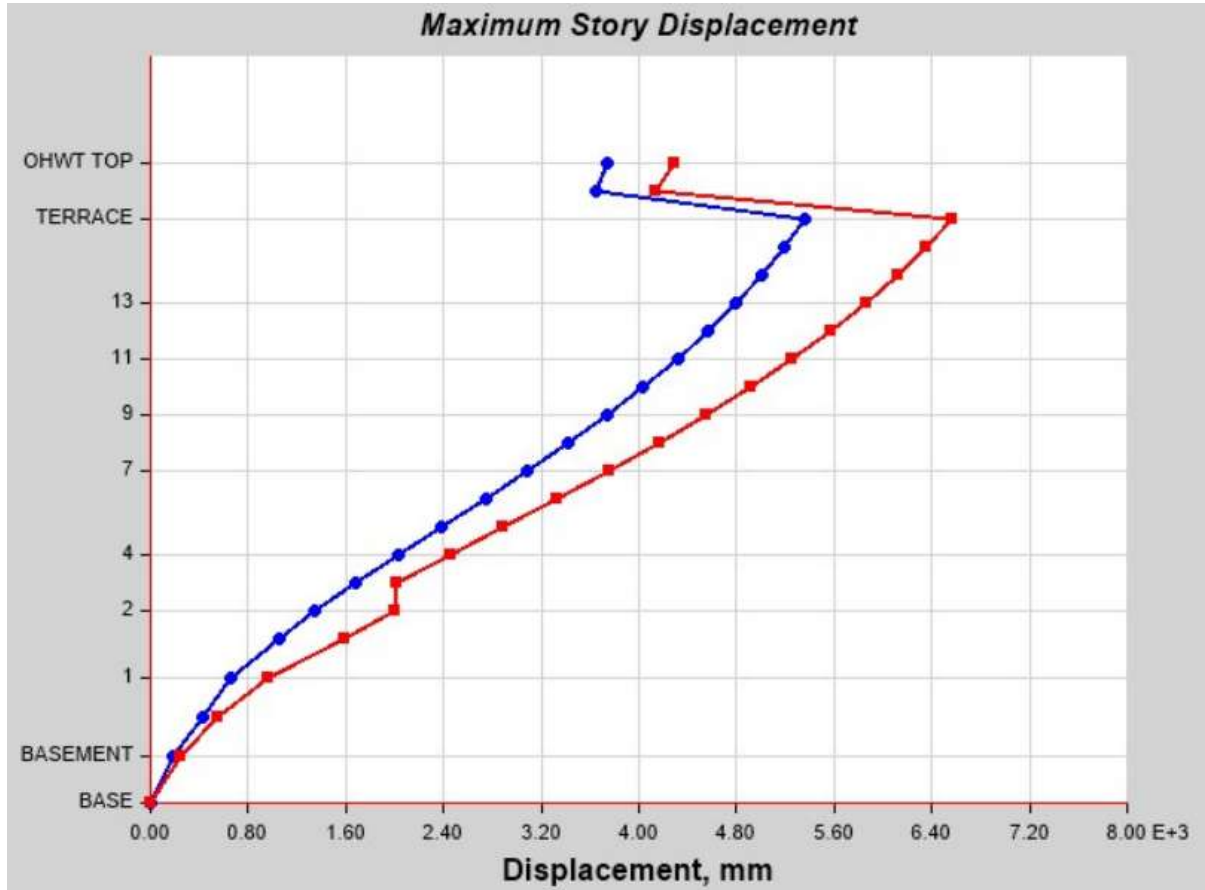
Table No. 3.13 Joint Displacement at Terrace for Combination 1.5(DL+EQX) (G+15)

TABLE: Joint Displacements									
Story	Label	Unique Name	Load Case/Combo	UX	UY	UZ	RX	RY	RZ
				mm	mm	mm	rad	rad	rad
TERRACE	15	151	3) 1.5(DL+EQX)	205.421	-63.072	-8.104	-0.00017	0.002581	0.006652
TERRACE	15	151	ENV Max	205.421	91.401	-0.785	0.001339	0.002581	0.006755
TERRACE	26	3424	3) 1.5(DL+EQX)	205.256	55.511	-18.815	-0.00015	0.002684	0.006426
TERRACE	26	3424	ENV Max	205.256	102.644	-2.005	0.002441	0.002684	0.006571

Table No. 3.14 Joint Displacement at Terrace for Combination 0.9DL+1.5WLX+TH Max) (G+15)

TABLE: Joint Displacements									
Story	Label	Unique Name	Load Case/Combo	UX	UY	UZ	RX	RY	RZ
				mm	mm	mm	rad	rad	rad
TERRACE	15	151	0.9DL+1.5WLX+TH Max	5468.802	2486.216	121.517	0.064011	0.057572	0.394671
TERRACE	26	3424	0.9DL+1.5WLX+TH Max	5468.549	5852.678	158.219	0.105521	0.05825	0.390071
TERRACE	15	151	0.9DL-1.5WLY+TH Max	5415.733	2443.237	119.022	0.064732	0.056969	0.392826
TERRACE	26	3424	0.9DL-1.5WLY+TH Max	5415.441	5776.502	157.97	0.106509	0.057634	0.388228

Graph No.6 Displacement v/s Storey for G+15



3.6.3 Drift

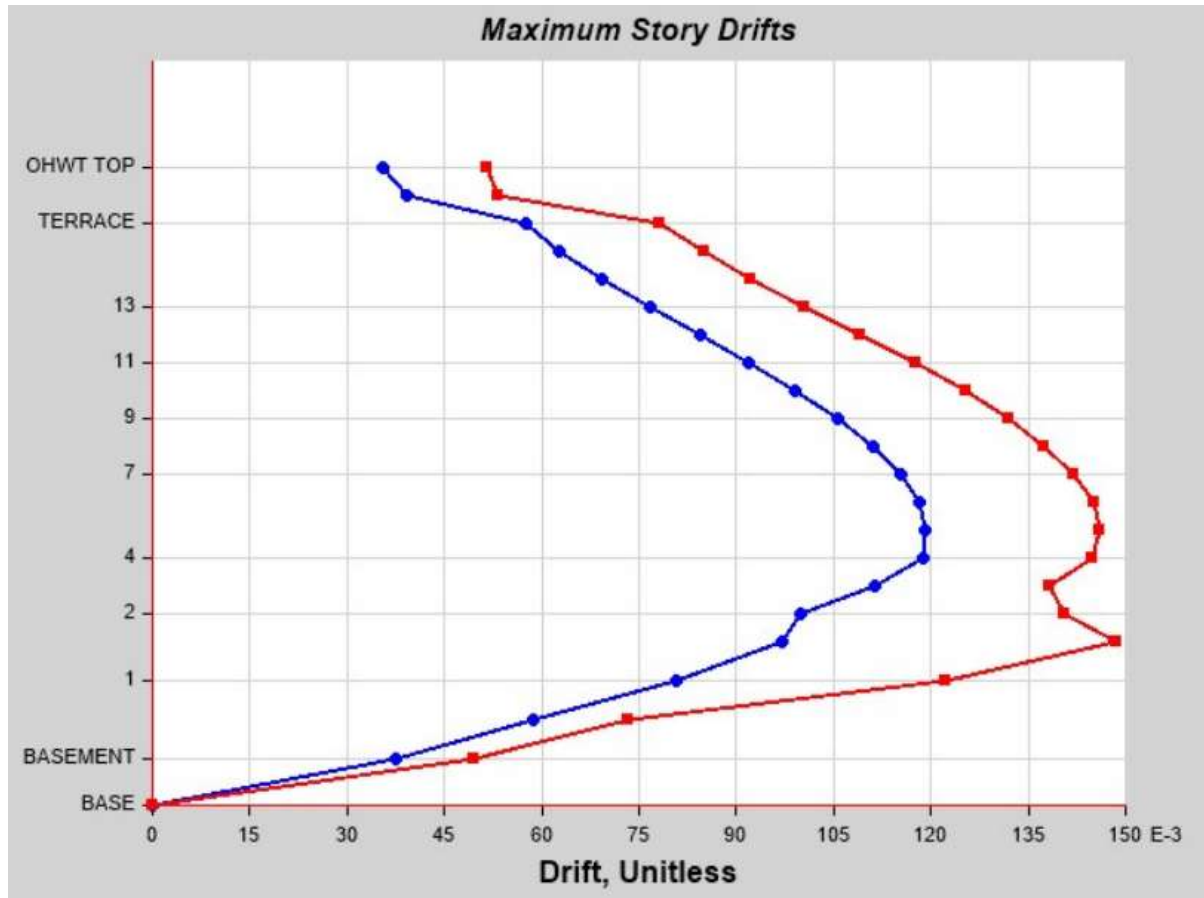
Table No. 3.15 Storey Drift for 1.5(DL+EQX)combination (G+15)

TABLE: Story Drifts				
Story	Load Case/Combo	Direction	Drift	Label
6	3) 1.5(DL+EQX)	X	0.004363	14

Table No. 3.16 Storey Drift for 0.9DL-1.5WLY+TH Min combination (G+15)

TABLE: Story Drifts				
Story	Load Case/Combo	Direction	Drift	Label
5	0.9DL-1.5WLY+TH Min	Y	0.184393	46

Graph No.7 Drift v/s Storey for G+15



IV. RESULT

- The blast pressure intensity for 0.3,0.6,0.9,1,1.2,1.5,1.8 sec's are 2.355,2.09,1.83,1.57,1.3,0.78,0.26 Mpa respectively.
- Analatical results for G+24,G+18,G+15 building are as follows:
In post analysis result it can be seen that prior to the blast impact the building was structurally sound & stable with 48.46% & 64.53% mass participation in first 2 mode with minimum torsion of 15%.
- The maximum terrace displacement prior to the blast was 204.24mm (0.9DL + 1.5WL)which considerably low and under the allowable displacement as per IS standards but after appling Time History Analysis it showed tremendous change in results as it went to 13.247m(0.9dl+1.5wlx+TH).
- The storey drift was 0.309 also considerable high after the blast.
- For G+18 the results were proportionally less as compared to higher G+24 building. The displacement was 7.5m which is almost half the displacement in G+24 after the blast.

- Here, we can say that the deformation was less in G+18 as compared with G+24.
- Moving forward for the same pressure intensity the response of G +15 was also computed the displacement before the blast in G+15 was 205.421mm(1.5DL+EQx) and after the blast it was 5.46m which is considerably low when compared with G+18 & G+24.
- The mass participation factor was more over same in all 3 cases but torsion was high by 2% in G+15 i.e 17%.

V. CONCLUSION

- The blast analysis on a high rise structure is one the less researched subject. This thesis helps us understand how a blast affects a building and how the results can be computed by using FEM based models.
- During the research we found the deformation of the building takes place by shockwaves which is created due to the blast and how the pressure intensity varies w.r.t the time in sec.
- At the start, the shockwave affects the building tremendously as shown in table 3.1and as the time progress the shock waves wares off.

- The research have come across that the height of the building plays an important role in resulting damage due to the shockwaves and Hence we can conclude that the height of the building is directly proportional to the damage it is subjected to.
- Moving further, In areas which are more prone to the terrorist attacks and the building which are Important to the nation w.r.t its stable economy should be considered for the blast analysis.
- Few international standard codes gives the provision which will help the building to be integrally strong during such blast.
- In case of G+15 building, if provided with the lateral bracing and using a high grade of material the damage can be controlled to a certain extend and the damage can be rectified by some local repairs itself. The research further can be continued by performing a high scale experiments on the provided remedial measures which might require some high resources.

REFERENCE

- [1]. Prediction of blast loading and its impact on buildings, Nitesh n. Moon
- [2]. Prediction Concrete Structures Subjected to Blast Loading Fracture due to dynamic response, Jonas Ekstrom
- [3]. Response of buildings exposed to blast load method evaluation, Per-erikaustrell
- [4]. A review of methods for predicting bomb blast effects on buildings, Alexander M. Remennikov,
- [5]. Column load balancing in prestressed concrete building, By S. L. Lee,1 Fellow, ASCE, S. Tumilar,2 Member, ASCE, and H. C. Chin3
- [6]. Serviceability Performance of Prestressed Concrete Buildings Taking into Account Long Term Behaviour and Construction Sequence H. L. YIP, F. T. K. AU, S. T. SMITH
- [7]. The analysis of prestressed concrete structures and the application of recent research by peter beaumontmorice, b.sc., ph.d., a.m.i.c.e.
- [8]. Experimental and numerical study on the performance of externally prestressed reinforced high strength concrete beams with openings Ahmed M. El-Basiouny1, Hamed S. Askar1 Mohamad E,El-Zoughiby
- [9]. Building structure failures caused by accidental loads
- [10]. Accidental Eccentricity of Story Shear for Low-Rise Office Buildings Jaime De-la-Colina; Bernardino Benítez; and Sonia E. Ruiz
- [11]. Estimation of Accidental Torsion Effects for Seismic Design of Buildings Juan C. De la Llera, Anil K. Chopra,
- [12]. Determining Appropriate Design Impact Loads to Roadside Structures Using Stochastic Modeling Ivar Björnsson; Sven Thelander; and Fredrik Carlsson
- [13]. Jun Yu; Tassilo Rinder; Alexander Stolz; Kang-Hai Tan, Dynamic Progressive Collapse of an RC Assemblage Induced by Contact Detonation (2008)
- [14]. Youpo Su, Ying Tian, University of Nevada, Las Vegas, Progressive Collapse Resistance of Axially-Restrained Frame Beams, *ACI Structural Journal* 106(5):600-607, September (2009)
- [15]. Meng-Hao Tsai, Effect of Interior Brick-infill Partitions on the Progressive Collapse Potential of a RC Building: Linear Static Analysis Results Article, February (2009)
- [16]. Ahmed Atta and Mohamed Taman, Using high-performance cementitious mortar and external prestressing for retrofitting of corroded reinforced concrete beams, *Advances in Structural Engineering* (2020)
- [17]. V. Kumar, M. A. Iqbal", A. K. Mittal, Behaviour of prestressed concrete under drop impact loading, 11th International Symposium on Plasticity and Impact Mechanics, 20 (2017)
- [18]. Ahmed Atta and Mohamed Taman, PROGRESSIVE COLLAPSE, METHODS OF PREVENTION, Saimaa University of Applied Sciences (2013)
- [19]. Tao Yang, Wanqing Chen, and Zhongqing Han, Research Article Experimental Investigation of Progressive Collapse of Prestressed Concrete Frames after the Loss of Middle Column (2020)
- [20]. Qian Kai, Feng Fu, Progressive Collapse Resistance of Precast Concrete Beam-Column Subassemblages with High-Performance Dry Connections (2019)
- [21]. Hou Jian, Ph.D.; Song Li, Ph.D.; and Liu Huanhuan, Testing and Analysis on Progressive Collapse-Resistance Behavior of RC Frame Substructures under a Side Column Removal Scenario (2016)

- [22]. S. M. Marjanishvili, P.E., M. ASCE, Progressive Analysis Procedure for Progressive Collapse
- [23]. John Abruzzo; Alain Matta, Ph.D.; and Gary Panariello, Ph.D, Study of Mitigation Strategies for Progressive Collapse of a Reinforced Concrete Commercial Building
- [24]. Jun Yu, Kang-Hai Tan, Special Detailing Techniques to Improve Structural Resistance against Progressive Collapse (2014)
- [25]. Mehrdad Sasani and Serkan Sagiroglu, Gravity Load Redistribution and Progressive Collapse Resistance of 20-Story Reinforced Concrete Structure following Loss of Interior Column (2010)
- [26]. Kai Qian, M.ASCE; Yun-Hao Weng; and Bing Li, M.ASCE, Improving Behavior of Reinforced Concrete Frames to Resist Progressive Collapse through Steel Bracings
- [27]. Rohit B. Nimse, Digesh D. Joshi, Paresh V. Patel Behavior of wet precast beam column connections under progressive collapse scenario: an experimental study
- [28]. Kai, Qian; Li, Bing Slab effects on response of reinforced concrete substructures after loss of corner column (2012)
- [29]. Qian, Kai; Li, Bing, Investigation into resilience of precast concrete floors against progressive collapse (2019)
- [30]. JianwuPan , Xian Wang , and Fang Wu, Strengthening of Precast RC Frame to Mitigate Progressive Collapse by Externally Bonded CFRP Sheets Anchored with HFRP Anchors (2018)
- [31]. Spencer E. Quiel, Clay J. Naito, Corey T. Fallon A non-emulative moment connection for progressive collapse resistance in precast concrete building frames (2019)